Am J Transl Res 2020;12(5):2118-2135
www.ajtr.org /ISSN:1943-8141/AJTR0105665

Original Article

Long non-coding RNA MVIH promotes cell proliferation, migration, invasion through regulating multiple cancer-related pathways, and correlates with worse prognosis in pancreatic ductal adenocarcinomas

Shaobo Hu[1], Qichang Zheng[1], Jiongxin Xiong[2], Heshui Wu[2], Weici Wang[3], Wei Zhou[2]

Departments of [1]Hepatobiliary Surgery, [2]Pancreatic Surgery, [3]Vascular Surgery, Union Hospital, Tongji Medical College, Huazhong University of Science and Technology, Wuhan, China

Received November 29, 2019; Accepted April 24, 2020; Epub May 15, 2020; Published May 30, 2020

Abstract: We aimed to explore the effect of long non-coding RNA MVIH (lnc-MVIH) on cell proliferation, migration as well as invasion, and investigate the landscape of its molecular mechanism in pancreatic ductal adenocarcinomas (PDAC). Control overexpression (OE-NC group) and lnc-MVIH overexpression (OE-MVIH group) plasmids were transfected in BxPC-3 cells; control knock-down (KD-NC group) and lnc-MVIH knock-down (KD-MVIH group) plasmids were transfected in PANC-1 cells. Cellular functions were measured and mRNA sequencing was conducted. In 70 PDAC patients, lnc-MVIH expression in tumor and adjacent tissues was detected. Lnc-MVIH expression was higher in human PDAC cell lines than human normal pancreatic ductal epithelial cell line. Cell proliferation, migration and invasion were increased in OE-MVIH group compared to OE-NC group, but decreased in KD-MVIH group compared to KD-NC group. mRNA sequencing showed 145 differentially expressing genes (DEGs) upregulated in OE-MVIH group *vs.* OE-NC group and downregulated in KD-MVIH group *vs.* KD-NC group, and 51 DEGs downregulated in OE-MVIH group *vs.* OE-NC group and upregulated in KD-MVIH group *vs.* KD-NC group. These DEGs were enriched in several cancer-related pathways (including Hippo signaling pathway, cell cycle, Forkhead box O signaling pathway, apoptosis and advanced glycation end products-RAGE signaling pathway), and the effect of lnc-MVIH on regulating these DEGs was further validated by RT-qPCR. In PDAC patients, lnc-MVIH expression was increased in tumor tissue and correlated with advanced tumor size, lymph node metastasis, TNM stage and poor OS. In conclusion, lnc-MVIH might be a potential therapeutic target which regulated multiple cancer-related pathways in PDAC.

Keywords: Long non-coding RNA MVIH, pancreatic ductal adenocarcinomas, cellular function, mRNA sequencing, prognosis

Introduction

Pancreatic cancer (PC), one of the most aggressive solid malignancies, remains the seventh leading cause of cancer-related death globally in 2018 and is predicted to be the second leading cause of cancer-related death, ranked after lung cancer, by 2030 [1, 2]. As one of the most common types of PC, pancreatic ductal adenocarcinomas (PDAC) constitutes approximately 95% of all PC cases [3]. Currently, surgical resection is the most optimally curative treatment for PDAC, while nearly 80%-90% of PDAC patients are not applicable for this curative option due to local invasion and distant metastasis [4]. Except surgical resection, therapeutic options include chemotherapy, radiation, immunotherapy as well as targeted drugs, whereas these therapies are palliative for relieving disease relevant symptoms and prolonging survival to some extent [1]. More importantly, despite the great improvement of novel treatments and individual care in last few decades, there is still no obvious improvement of prognosis with 5-year survival rate of approximately 5-7% in PDAC patients [4]. Hence, deeper understanding for molecular mechanisms underlying PDAC and investigations for its novel therapeutic targets are urgently required, which might provide new insights into the biology of PDAC and improve the prognosis.

Long non-coding RNAs (lncRNAs), a class of noncoding RNAs (>200 nt in length) without protein-coding capacity, participate in multiple biological processes, including epigenetics, RNA alternative splicing, RNA degradation, X chromatin inactivation and chromatin remodeling [5, 6]. As one of the newly found lncRNAs, lncRNA associated with microvascular invasion in hepatocellular carcinoma (lnc-MVIH) is highly expressed in hepatocellular carcinoma (HCC), and is capable to enhance tumor-inducing angiogenesis via inhibiting the secretion of phospho-glycerate kinase 1 (PGK1) as well as promote tumor growth [7, 8]. Apart from HCC, it also has been reported to be upregulated in several cancers (such as breast cancer and lung cancer), and contribute to the processes of microvascular invasion as well as the promotion of cell proliferation, invasion and migration in cancers [7, 9-11].

Considering that lnc-MVIH serves as a tumor promoter via stimulating cell growth, migration as well as invasion, and enhancing tumor angiogenesis in several carcinomas, we supposed that lnc-MVIH might play as a tumorigenic factor in PDAC as well. Whereas the detailed molecular mechanism of lnc-MVIH underlying PDAC and its influence on disease progression and prognosis in PDAC patients are still unclear. Hence, we performed a preliminary study with a small sample size, we discovered that lnc-MVIH expression was increased in tumor tissue compared to adjacent tissue, and it was correlated with advanced diseases conditions in PDAC patients. Based on the above mentions, the purpose of this study was to assess the effect of lnc-MVIH on cell proliferation, apoptosis, migration as well as invasion, to explore the landscape of its molecular mechanism in PDAC, also to investigate its correlation with clinical features and prognosis in PDAC patients.

Materials and methods

Cell culture

Human PDAC cell lines PSN-1, AsPC-1, PANC-1 and BxPC-3, which were purchased from ATCC (VA, USA), were cultured in 90% RPMI-1640 medium with 10% fetal bovine serum (FBS) (Hyclone, USA). The human normal pancreatic ductal epithelial cell line H6C7 (Kerafast, USA) was maintained in serum free Keratinocyte Basal Medium (KBM) fortified with growth factors, cytokines, and supplements (SingleQuots™ Kit, Lonza, Switzerland) in accordance with manufacturer's manual. lnc-MVIH expression in these cells was evaluated by Reverse Transcription Quantitative Polymerase Chain Reaction (RT-qPCR).

Plasmid transfection

PEX-2 vector was applied to construct control overexpression plasmids and lnc-MVIH overexpression plasmids, and pGPH1 vector was used to structure control knock-down plasmids and lnc-MVIH knock-down plasmids. BxPC-3 cells were transfected with control and lnc-MVIH overexpression plasmids, which were named as OE-NC group and OE-MVIH group respectively. PANC-1 cells were transfected with control and lnc-MVIH knock-down plasmids, which were then named as KD-NC group and KD-MVIH group. RT-qPCR was performed to assess the expression of lnc-MVIH in four groups at 24 h post transfection. Cell proliferation determination was carried out at 0 h, 24 h, 48 h and 72 h, with cell counting kit-8 (CCK-8, Dojindo, USA) in terms of operating Instructions of the kit. Cell apoptosis detection was conducted by Annexin V/Propidium Iodide (AV/PI) assay at 48 h with the use of Annexin V-FITC Apoptosis Detection Kit (R&D, USA) following instruction for use. Cell migration assessment was conducted at 48 h by wound scratch assay, and invasion ability measurement was performed at 48 h using transwell assay as previously described [12].

Chemosensitivity assay

After plasmids transfection, cells were cultured with various concentrations of Gemcitabine (Sigma, USA) or 5-Fluorouracil (5-FU) (Sigma, USA) for 48 h. Subsequently, cell viability was detected by CCK-8 (Dojindo, USA) in terms of operating Instructions of the kit. In BxPC-3 cells, the concentration of Gemcitabine was 0, 0.25, 0.5, 1, 2, 4 and 8 μM; the concentration of 5-FU was 2, 2, 4, 8, 16, 32, and 64 μM. In PANC-1 cells, the concentration of Gemcitabine was 0, 5, 10, 20, 40, 80 and 160 μM; the concentration of 5-FU was 0, 20, 40, 80, 160, 320 and 640 μM.

RNA sequencing and bioinformatics

At 48 h after transfection, OE-NC, OE-MVIH, KD-NC and KD-MVIH cells were collected for

Table 1. Five key cancer-related pathways in KEGG enrichment analysis of accordant DEGs

Path term	Num of symbols	Proportion of symbols	Symbols	Fold enrichment	*P* value
Hippo signaling pathway	7	0.076	BIRC5, AREG, SMAD4, PRKCZ, SNAI2, TGFB2, FZD4	3.994	0.003
Cell cycle	7	0.076	SMAD4, BUB1, BUB1B, TGFB2, CCNB2, CDK1, CDC20	4.340	0.005
FoxO signaling pathway	6	0.065	SMAD4, BCL6, SOD2, TGFB2, TNFSF10, CCNB2	3.442	0.028
Apoptosis	5	0.054	DAXX, DFFA, BIRC5, TUBA4A, TNFSF10	3.295	0.033
AGE-RAGE signaling pathway	5	0.054	F3, ICAM1, SMAD4, PRKCZ, TGFB2	3.806	0.040

KEGG: Kyoko Encyclopedia of Genes and Genomes; DEG: differentially express gene.

RNA sequencing (RNA-Seq). Briefly, after extraction with PureZOL RNA isolation reagent (Bio-Rad, USA), the integrity and concentration of RNA were assessed by Agilent 2100 Bioanalyzer (Agilent, USA). Then, the RNA-Seq library was generated by Genergy Bio (Shanghai, China) according to the methods described previously [13]. Trim_galore software was applied to trim poor-quality bases and adapter. Subsequently, trimmed reads were mapped to the human reference genome (hg38) using Tophat [14] with the default parameters and Ensemble genome annotation (Homo_sapiens.GRCh38.83.chr.gtf). Finally, the raw count of each gene was calculated by featurecount, and gene differential expression was estimated using DESeq2 [15]. For RNA-Seq data analysis, packages of R software were used for statistical analyses and graphs. Principal component analysis (PCA) of mRNA expression profile was performed by Factoextra package; heatmap of mRNA expression profile was plotted by pheatmap package. And mRNAs with a fold change (FC) ≥2.0 and an adjusted *P* value (BH multiple test correction) <0.05 were identified as differentially expressing genes (DEGs) and displayed using Volcano Plots. The overview about overlap of OE-DEGs and KD-DEGs was displayed in Venn diagram (VennDiagram package). Gene Ontology (GO) and Kyoko Encyclopedia of Genes and Genomes (KEGG) enrichment analyses of OE-DEGs, KD-DEGs as well as "accordant DEGs" were completed using DAVID web servers [16], where the "accordant DEGs" means the DEGs were up-regulated in OE-MVIH vs. OE-NC and down-regulated in KD-MVIH vs. KD-NC, or the DEGs were up-regulated in KD-MVIH vs. KD-NC and down-regulated in OE-MVIH vs. OE-NC. The GO enrichment and KEGG enrichment were illustrated in bubble diagram plotted by ggplot2 package in R.

Screening pathway

Through the KEGG enrichment analysis of the accordant DEGs, 5 key cancer-related pathways were screened out (shown in **Table 1**). Then in the cells of four groups (OE-NC, OE-MVIH, KD-NC and KD-MVIH), RT-qPCR was conducted to further validate the mRNA relative expression of genes implicated in these 5 cancer-related pathways.

Tumor and adjacent specimen collection

A total of 70 PDAC patients underwent resection in Union hospital from July 2015 to June 2018 were recruited in this study. The current study was approved by the Institutional Review Board of Union hospital, and all patients signed the informed consents. All enrolled patients were elder than 18 years and pathologically diagnosed as primary PDAC. The tumor tissue and adjacent tissue of patients were collected from surgical resection, which were immediately stored in liquid nitrogen after resection, then used for the detection of the lnc-MVIH expression by RT-qPCR. Besides, patients' clinical characteristics (age, gender, history of smoke and drink, tumor site, pathological grade, tumor size, lymph node metastasis, and TNM Stage) were documented, and all patients were followed up to June 2018 for the assessment of OS.

RT-qPCR

Total RNA was extracted using PureZOL RNA isolation reagent (Bio-Rad, USA). After that, 1 ug RNA was reversely transcribed to cDNA using RT-PCR Quick Master Mix (Toyobo, Japan). qPCR was carried out by KOD SYBR® qPCR Mix (Toyobo, USA). The PCR amplification were performed as follows: 95°C for 5 min, followed by 40 cycles of 95°C for 5 s, 61°C for 30 s. Calculation was finished by using $2^{-\Delta\Delta Ct}$. GAPDH was used as an internal reference. Primers were listed in Supplementary Table 1.

Statistical analysis

Data processing and statistical analysis were performed on SPSS 20.0 (IBM, USA) and

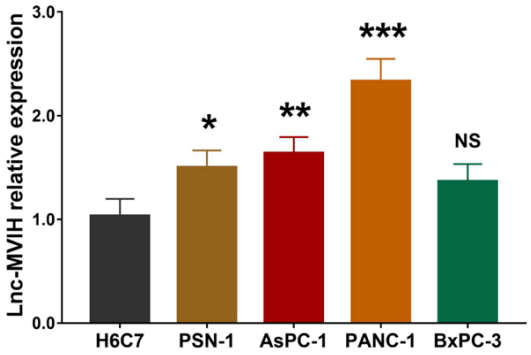

Figure 1. Lnc-MVIH expression was higher in most human PDAC cell lines compared to human normal pancreatic ductal epithelial cell line. Lnc-MVIH: long non-coding RNAs associated with microvascular invasion in hepatocellular carcinoma; PDAC: pancreatic ductal adenocarcinomas.

GraphPad Prism 7.01 (GraphPad Software, USA). Continuous data were described as mean with standard deviation (SD), or median and interquartile range (IQR), or displayed as scatter plot or bar graph with error bars. Categorical data were presented as number (percentage). Comparison of continuous data between two groups was determined by the unpaired t test, while comparison of paired continuous data was determined by Wilcoxon signed-rank test. Comparison of continuous data among groups was determined by One-way ANOVA followed by Dunnett's multiple comparisons. Comparison of categorical data between two groups was determined by Chi-square test. OS was calculated from the date of surgical resection to the date of death, while the patients who lost follow-up or not known to have died at last follow-up were censored on the date that they were last known to be alive. The OS were displayed using Kaplan-Meier curve, and comparison of OS between two groups were determined by the log-rank test. Predictors for OS were assessed by the Cox's proportional hazards model analysis. *P* value <0.05 indicated statistically significant. The "NS", "*", "**", and "***" in the figures respectively represented the *P* value >0.05 (no significance), *P* value <0.05, *P* value <0.01, and *P* value <0.001.

Results

Lnc-MVIH expression in human PDAC cell lines and human normal pancreatic ductal epithelial cell line

Lnc-MVIH expression was higher in human PDAC cell lines PSN-1 ($P<0.05$), AsPC-1 ($P<0.01$) as well as PANC-1 ($P<0.05$), but was similar in BxPC-3 ($P>0.05$) compared with human normal pancreatic ductal epithelial cell line H6C7 (**Figure 1**). Subsequently, BxPC-3 cells and PANC-1 cells were selected in the following assays.

Effect of lnc-MVIH on cell proliferation and cell apoptosis

In BxPC-3 cells, lnc-MVIH expression was higher in OE-MVIH group compared to OE-NC group, suggesting the successful transfection (**Figure 2A**). Cell proliferation was increased in OE-MVIH group compared to OE-NC group at 48 h ($P<0.05$) and 72 h ($P<0.01$) (**Figure 2B**). Cell apoptosis was decreased in OE-MVIH group compared to OE-NC group at 48 h ($P<0.01$) (**Figure 2C**, **2D**). In PANC-1 cells, lnc-MVIH expression was lower in KD-MVIH group compared to KD-NC group, suggesting the successful transfection (**Figure 2E**). Cell proliferation was reduced in KD-MVIH group compared to KD-NC group at 48 h ($P<0.05$) and 72 h ($P<0.05$) (**Figure 2F**). Cell apoptosis was enhanced in KD-MVIH group compared to KD-NC group at 48 h ($P<0.01$) (**Figure 2G**, **2H**).

Effect of lnc-MVIH on cell migration and cell invasion

In BxPC-3 cells, cell migration was increased in OE-MVIH group compared to OE-NC group ($P<0.01$) (**Figure 3A**, **3B**). Cell invasion was enhanced in OE-MVIH group compared to OE-NC group ($P<0.01$) (**Figure 3C**, **3D**). In PANC-1 cells, cell migration was reduced in KD-MVIH group compared to KD-NC group ($P<0.05$) (**Figure 3E**, **3F**). Cell invasion was decreased in KD-MVIH group compared to KD-NC group as well ($P<0.01$) (**Figure 3G**, **3H**).

Effect of lnc-MVIH on cell chemosensitivity

In BxPC-3 cells, lnc-MVIH overexpression reduced Gemcitabine chemosensitivity (**Figure 4A**) as well as 5-FU chemosensitivity (**Figure 4B**). In PANC-1 cells, lnc-MVIH knock-down increased Gemcitabine chemosensitivity (**Figure 4C**) as well as 5-FU chemosensitivity (**Figure 4D**).

PCA plots and heatmap analysis for mRNA expression profile

In order to deeply investigate about the comprehensive molecule mechanism of lnc-MVIH in PDAC pathogenesis, we performed RNA

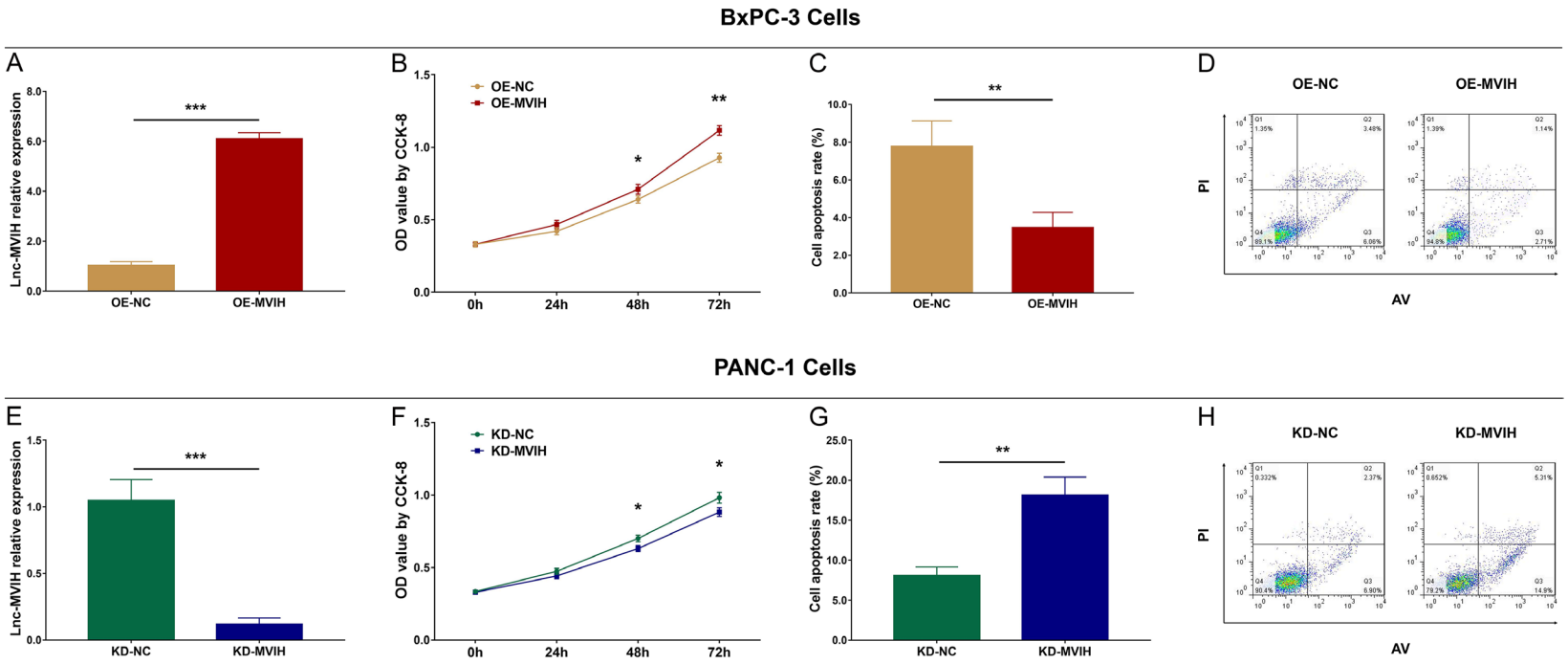

Figure 2. Lnc-MVIH promoted cell proliferation but inhibited apoptosis. In BxPC-3 cells, transfection was successful (A); cell proliferation was increased in OE-MVIH group compared to OE-NC group at 48 h and 72 h (B); cell apoptosis was decreased in OE-MVIH group compared to OE-NC group at 48 h (C, D). In PANC-1 cells, transfection was successful (E); Cell proliferation was reduced in KD-MVIH group compared to KD-NC group at 48 h and 72 h (F). Cell apoptosis was enhanced in KD-MVIH group compared to KD-NC group at 48 h (G, H). Lnc-MVIH: long non-coding RNAs associated with microvascular invasion in hepatocellular carcinoma. OD: optical density.

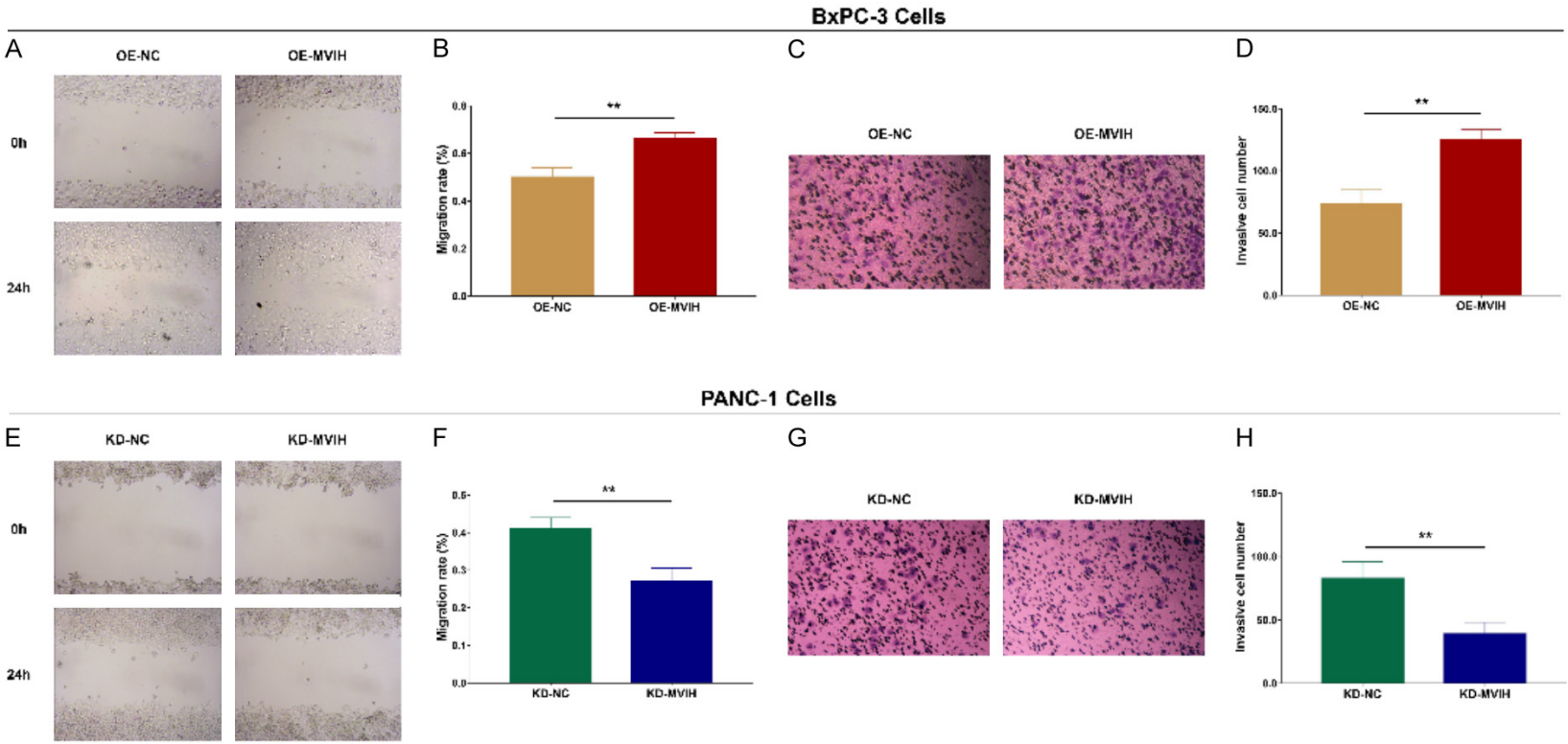

Figure 3. Lnc-MVIH promoted cell migration and increased cell invasion. In BxPC-3 cells, cell migration was increased in OE-MVIH group compared to OE-NC group (A, B); cell invasion was enhanced in OE-MVIH group compared to OE-NC group (C, D). In PANC-1 cells, cell migration was reduced in KD-MVIH group compared to KD-NC group (E, F); cell invasion was decreased in KD-MVIH group compared to KD-NC group as well (G, H). Lnc-MVIH: long non-coding RNAs associated with microvascular invasion in hepatocellular carcinoma.

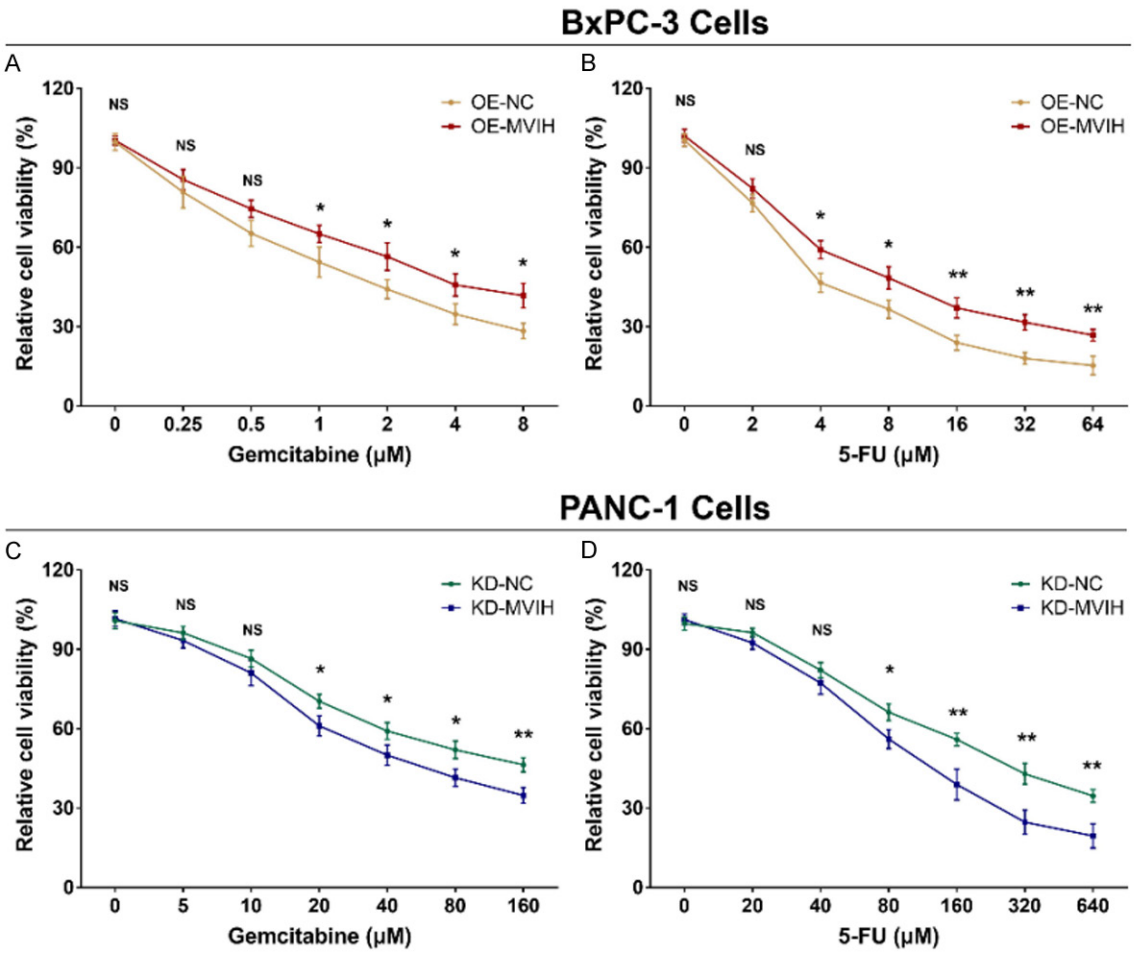

Figure 4. Lnc-MVIH reduced cell chemosensitivity. In BxPC-3 cells, lnc-MVIH overexpression reduced Gemcitabine chemosensitivity (A) and 5-FU chemosensitivity (B). In PANC-1 cells, lnc-MVIH knockdown increased Gemcitabine chemosensitivity (C) and 5-FU chemosensitivity (D). Lnc-MVIH: long non-coding RNAs associated with microvascular invasion in hepatocellular carcinoma; 5-FU: 5-Fluorouracil.

sequencing and bioinformatics in OE-NC, OE-MVIH, KD-NC and KD-MVIH cells. PCA plot (**Figure 5A**) and heatmap analyses (**Figure 5B**) of mRNA expression profile revealed that it was able to separate OE-MVIH group from OE-NC group, as well as distinguish KD-MVIH group from KD-NC group.

Volcano plot and Venn diagram analysis for dysregulated mRNAs

Volcano plot showed that there were 610 mRNAs up-regulated and 248 mRNAs down-regulated in the OE-MVIH group *vs.* OE-NC group (**Figure 6A**), and there were 709 mRNAs up-regulated and 501 mRNAs down-regulated in KD-MVIH group *vs.* KD-NC group (**Figure 6B**). Subsequently, we performed Venn diagram analysis that presented the overlapping patterns of DEGs in OE-MVIH group *vs.* OE-NC group and KD-MVIH group *vs.* KD-NC group. There were 196 accordant DEGs, containing 145 DEGs which were upregulated in OE-MVIH group *vs.* OE-NC group and downregulated in KD-MVIH group *vs.* KD-NC group, and 51 DEGs which were downregulated in OE-MVIH group *vs.* OE-NC group and upregulated in KD-MVIH group *vs.* KD-NC group (**Figure 6C**). In addition, 196 accordant DEGs detected by RNA-sequencing were shown in Supplementary Table 2.

GO and KEGG enrichment analyses for dysregulated mRNAs

In order to further explore the landscape of molecular mechanism of lnc-MVIH in PDAC, we performed enrichment analyses. For OE-DEGs

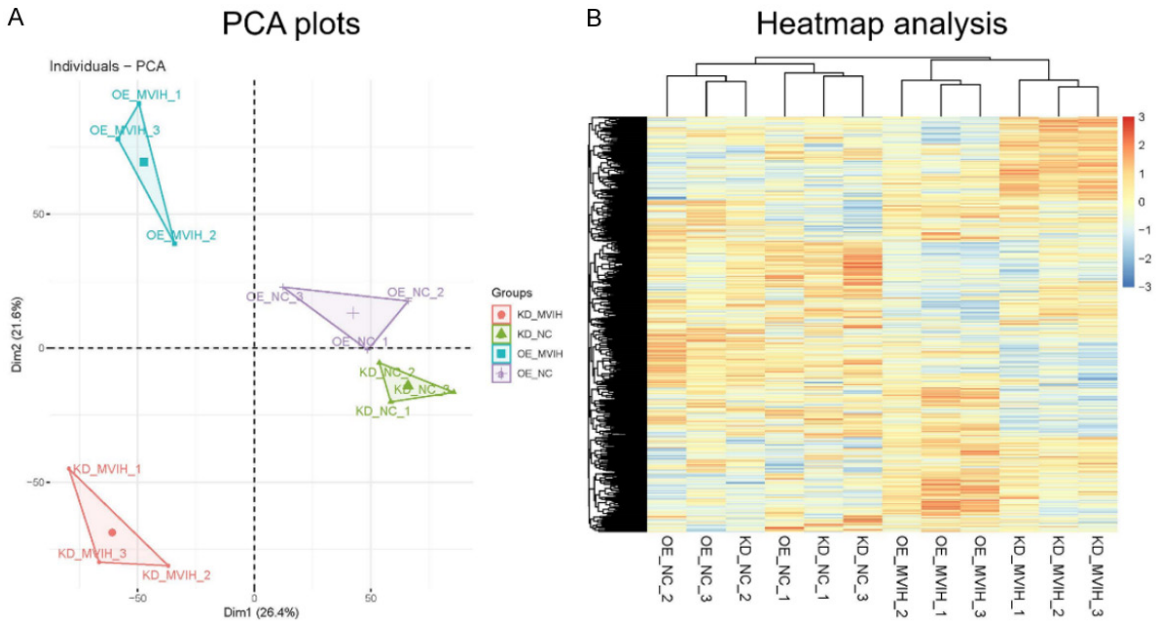

Figure 5. PCA plots and heatmap analysis. PCA plot of mRNA expression profiles (A); Heatmap analyses of mRNA expression profiles (B). PCA: principal component analysis.

(DEGs in OE-MVIH *vs.* OE-NC), GO enrichment analysis revealed that they were enriched in various biological processes (such as regulation of apoptotic process and response to drug), cellular components (such as plasma membrane and extracellular exosome) and molecular functions (such as protein binding and protein homodimerization activity) (**Figure 7A**). KEGG enrichment analysis disclosed that they were mainly were enriched in pathways in cancer, cytokine-cytokine receptor interaction and apoptosis and so on (**Figure 7B**). For KD-DEGs (DEGs in KD-MVIH vs. KD-NC), GO enrichment analysis displayed that they were enriched in several biological processes (such as regulation of cell cycle, defense response to virus and cell division), cellular component (such as cytoplasm and cytosol) and molecular functions (such as ATP binding and identical protein binding) (**Figure 7C**). KEGG enrichment analysis presented that they were enriched in cell cycle, cell adhesion molecules (CMAs) and p53 signaling pathway and so on (**Figure 7D**). For accordant DEGs, GO enrichment analysis found that they were enriched in a number of biological processes (such as positive regulation of proliferation, positive regulation of cell migration and regulation of cell cycle), cellular component (such as cytosol and cytoplasm) and molecular functions (such as protein binding, ATP binding and identical protein binding) (**Figure 7E**). KEGG enrichment analysis presented that they were enriched in several cancer-related pathways, such as Hippo signaling pathway, cell cycle, Forkhead box O (FoxO) signaling pathway, apoptosis and advanced glycation end products (AGE)-RAGE signaling pathway (**Figure 7F**).

Validation for 5 key cancer-related pathways

After the KEGG enrichment analysis of the accordant DEGs, 5 key cancer-related pathways (including Hippo signaling pathway, cell cycle, FoxO signaling pathway, apoptosis and AGE-RAGE signaling pathway) were screened out (**Table 1**). Subsequently, we further validated the relative expression of these accordant DEGs which were implicated in these 5 cancer-related pathways by RT-qPCR, and we found that most of these accordant DEGs were implicated in Hippo signaling pathway (**Figure 8A**), cell cycle (**Figure 8B**), FoxO signaling pathway (**Figure 8C**), apoptosis (**Figure 8D**) and AGE-RAGE signaling pathway (**Figure 8E**) were regulated by lnc-MVIH. These data indicated that lnc-MVIH might promote Hippo signaling pathway, cell cycle, FoxO signaling pathway and AGE-RAGE signaling pathway, but repress apoptosis to accelerate PDAC progression.

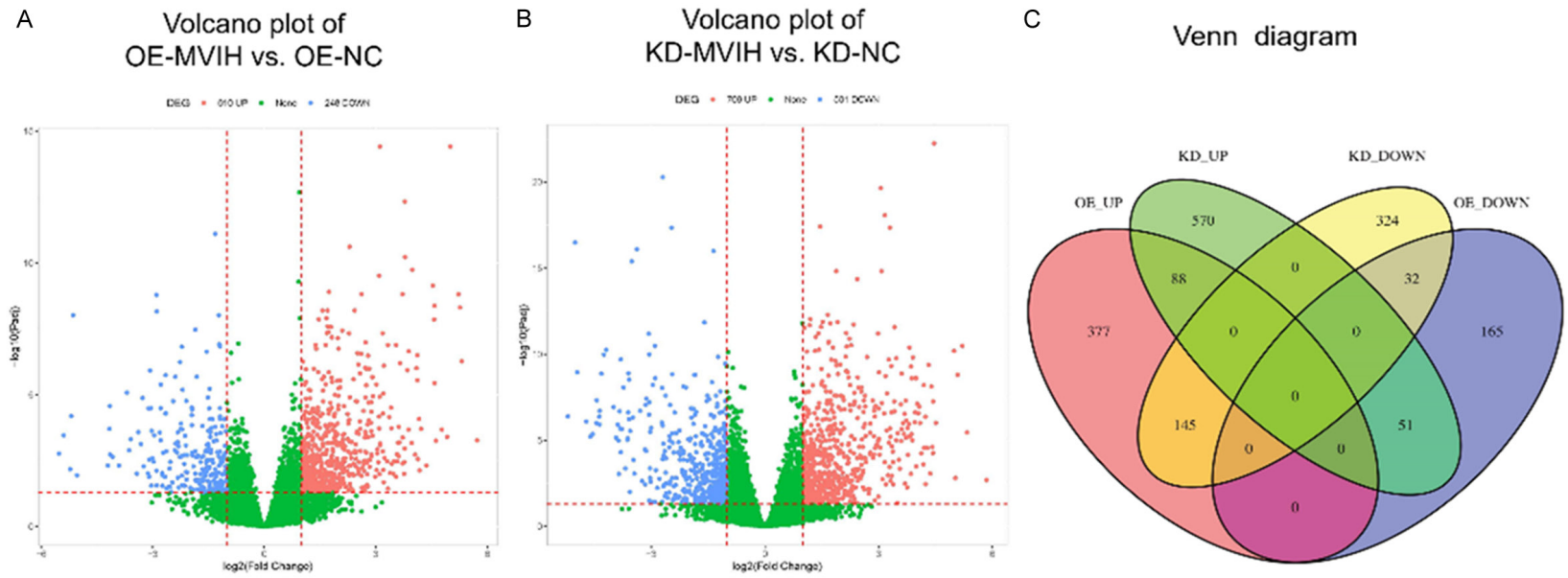

Figure 6. Volcano plot and Venn diagram analysis. Volcano plot for DEGs in the OE-MVIH group *vs.* OE-NC group (A); Volcano plot for DEGs in KD-MVIH group *vs.* KD-NC group (B); Venn diagram for DEGs in OE-MVIH group *vs.* OE-NC group and KD-MVIH group *vs.* KD-NC group (C). DEGs: differentially expressing genes.

A

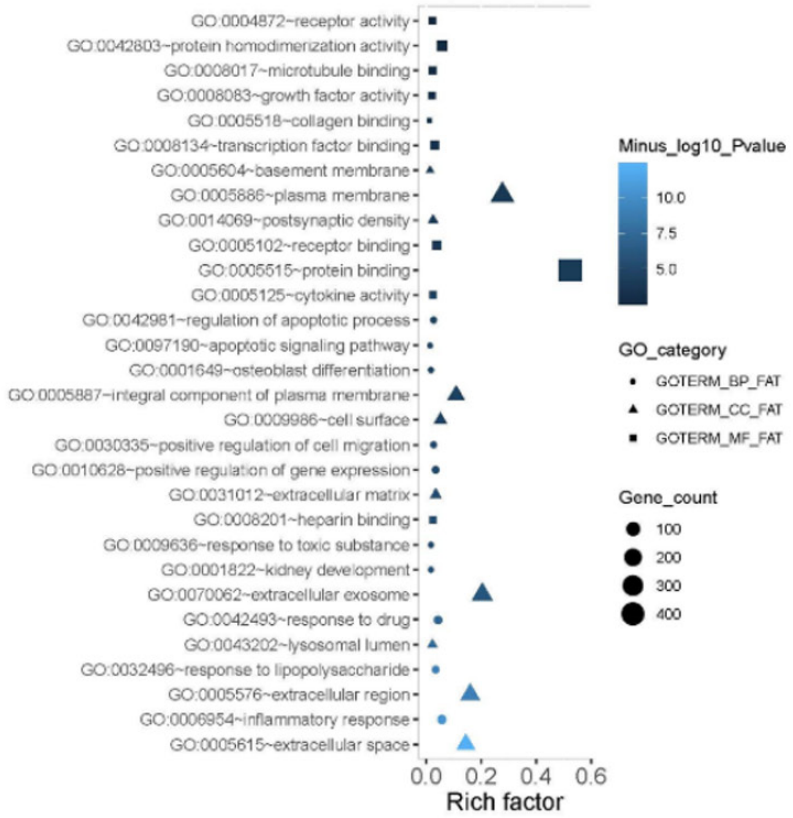
GO enrichment of OE-DEGs
GO:0004872~receptor activity
GO:0042803~protein homodimerization activity
GO:0008017~microtubule binding
GO:0008083~growth factor activity
GO:0005518~collagen binding
GO:0008134~transcription factor binding
GO:0005604~basement membrane
GO:0005886~plasma membrane
GO:0014069~postsynaptic density
GO:0005102~receptor binding
GO:0005515~protein binding
GO:0005125~cytokine activity
GO:0042981~regulation of apoptotic process
GO:0097190~apoptotic signaling pathway
GO:0001649~osteoblast differentiation
GO:0005887~integral component of plasma membrane
GO:0009986~cell surface
GO:0030335~positive regulation of cell migration
GO:0010628~positive regulation of gene expression
GO:0031012~extracellular matrix
GO:0008201~heparin binding
GO:0009636~response to toxic substance
GO:0001822~kidney development
GO:0070062~extracellular exosome
GO:0042493~response to drug
GO:0043202~lysosomal lumen
GO:0032496~response to lipopolysaccharide
GO:0005576~extracellular region
GO:0006954~inflammatory response
GO:0005615~extracellular space
0.0 0.2 0.4 0.6
Rich factor
Minus_log10_Pvalue
10.0
7.5
5.0
GO_category
GOTERM_BP_FAT
GOTERM_CC_FAT
GOTERM_MF_FAT
Gene_count
100
200
300
400

B

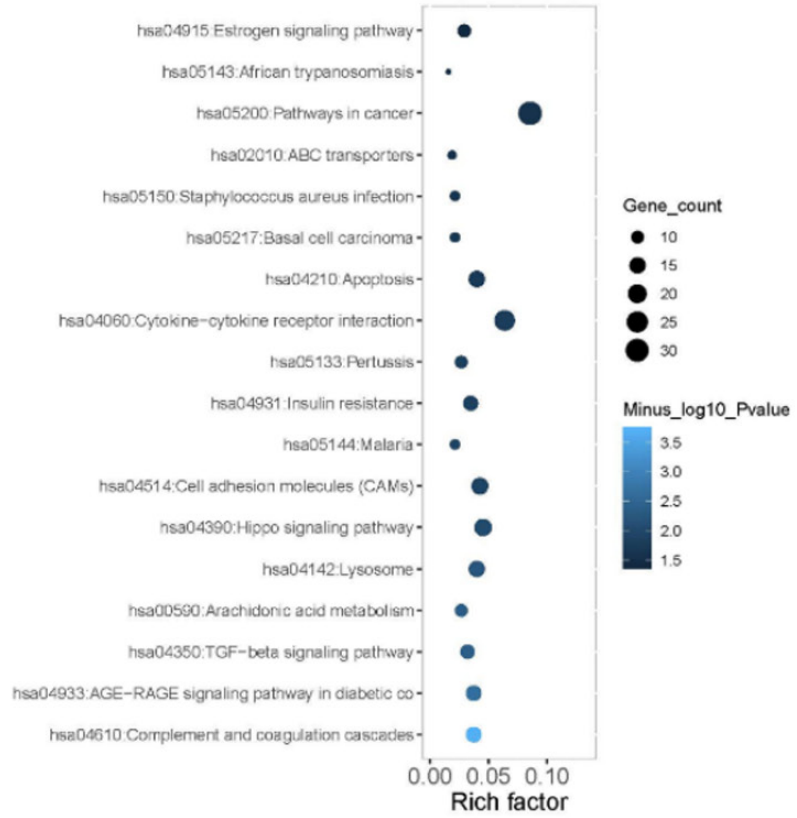
KEGG enrichment of OE-DEGs
hsa04915:Estrogen signaling pathway
hsa05143:African trypanosomiasis
hsa05200:Pathways in cancer
hsa02010:ABC transporters
hsa05150:Staphylococcus aureus infection
hsa05217:Basal cell carcinoma
hsa04210:Apoptosis
hsa04060:Cytokine−cytokine receptor interaction
hsa05133:Pertussis
hsa04931:Insulin resistance
hsa05144:Malaria
hsa04514:Cell adhesion molecules (CAMs)
hsa04390:Hippo signaling pathway
hsa04142:Lysosome
hsa00590:Arachidonic acid metabolism
hsa04350:TGF−beta signaling pathway
hsa04933:AGE−RAGE signaling pathway in diabetic co
hsa04610:Complement and coagulation cascades
0.00 0.05 0.10
Rich factor
Gene_count
10
15
20
25
30
Minus_log10_Pvalue
3.5
3.0
2.5
2.0
1.5

C

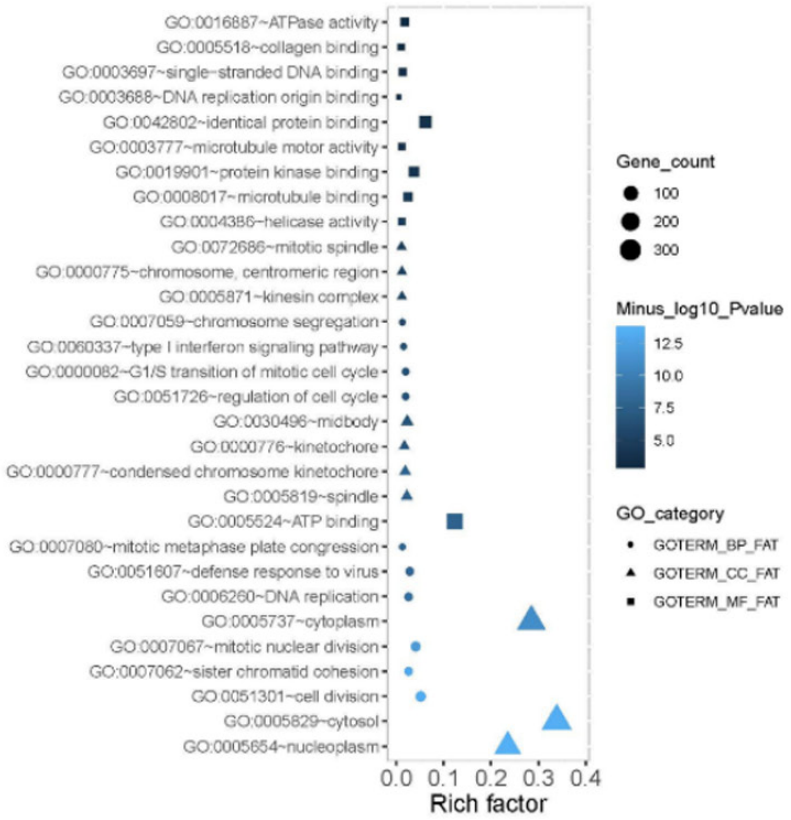
GO enrichment of KD-DEGs
GO:0016887~ATPase activity
GO:0005518~collagen binding
GO:0003697~single-stranded DNA binding
GO:0003688~DNA replication origin binding
GO:0042802~identical protein binding
GO:0003777~microtubule motor activity
GO:0019901~protein kinase binding
GO:0008017~microtubule binding
GO:0004386~helicase activity
GO:0072686~mitotic spindle
GO:0000775~chromosome, centromeric region
GO:0005871~kinesin complex
GO:0007059~chromosome segregation
GO:0060337~type I interferon signaling pathway
GO:0000082~G1/S transition of mitotic cell cycle
GO:0051726~regulation of cell cycle
GO:0030496~midbody
GO:0000776~kinetochore
GO:0000777~condensed chromosome kinetochore
GO:0005819~spindle
GO:0005524~ATP binding
GO:0007080~mitotic metaphase plate congression
GO:0051607~defense response to virus
GO:0006260~DNA replication
GO:0005737~cytoplasm
GO:0007067~mitotic nuclear division
GO:0007062~sister chromatid cohesion
GO:0051301~cell division
GO:0005829~cytosol
GO:0005654~nucleoplasm
0.0 0.1 0.2 0.3 0.4
Rich factor
Gene_count
100
200
300
Minus_log10_Pvalue
12.5
10.0
7.5
5.0
GO_category
GOTERM_BP_FAT
GOTERM_CC_FAT
GOTERM_MF_FAT

D

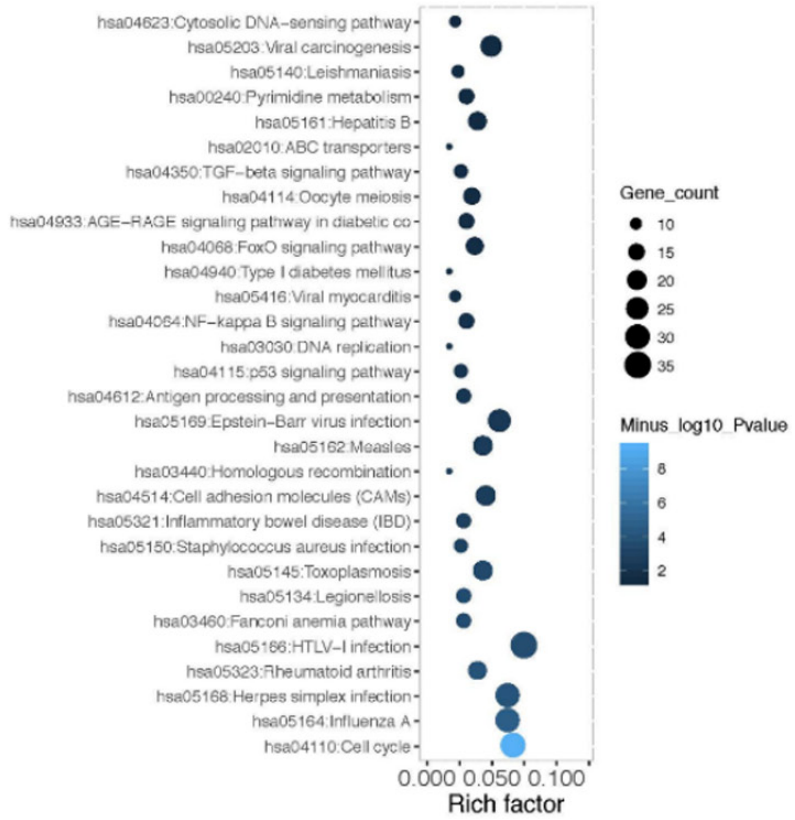
KEGG enrichment of KD-DEGs
hsa04623:Cytosolic DNA-sensing pathway
hsa05203:Viral carcinogenesis
hsa05140:Leishmaniasis
hsa00240:Pyrimidine metabolism
hsa05161:Hepatitis B
hsa02010:ABC transporters
hsa04350:TGF-beta signaling pathway
hsa04114:Oocyte meiosis
hsa04933:AGE-RAGE signaling pathway in diabetic co
hsa04068:FoxO signaling pathway
hsa04940:Type I diabetes mellitus
hsa05416:Viral myocarditis
hsa04064:NF-kappa B signaling pathway
hsa03030:DNA replication
hsa04115:p53 signaling pathway
hsa04612:Antigen processing and presentation
hsa05169:Epstein-Barr virus infection
hsa05162:Measles
hsa03440:Homologous recombination
hsa04514:Cell adhesion molecules (CAMs)
hsa05321:Inflammatory bowel disease (IBD)
hsa05150:Staphylococcus aureus infection
hsa05145:Toxoplasmosis
hsa05134:Legionellosis
hsa03460:Fanconi anemia pathway
hsa05166:HTLV-I infection
hsa05323:Rheumatoid arthritis
hsa05168:Herpes simplex infection
hsa05164:Influenza A
hsa04110:Cell cycle
0.000 0.050 0.100
Rich factor
Gene_count
10
15
20
25
30
35
Minus_log10_Pvalue
8
6
4
2

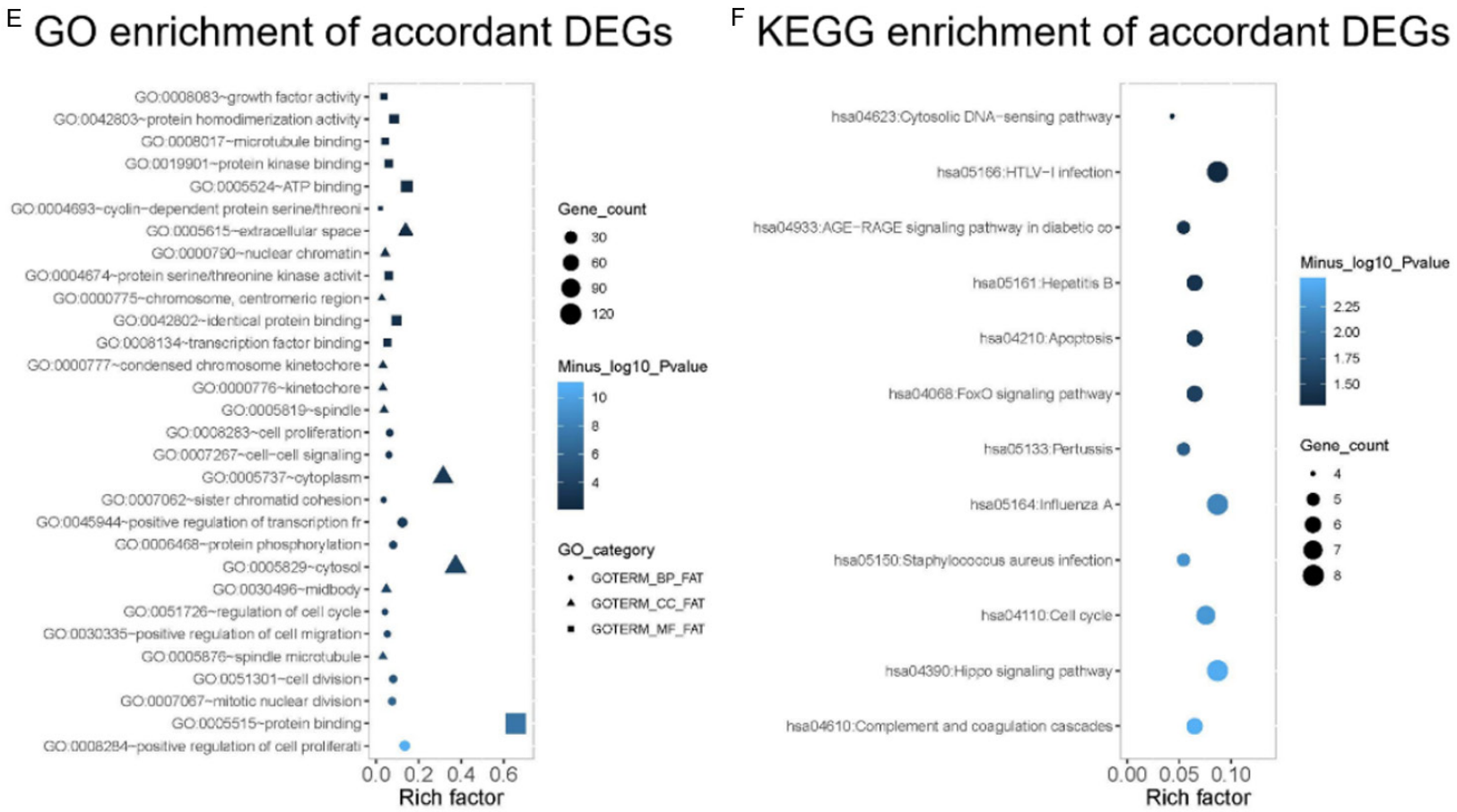

Figure 7. GO and KEGG enrichment analyses. GO enrichment analysis (A) and KEGG enrichment analysis (B) of OE-DEGs (DEGs in OE-MVIH group *vs*. OE-NC group); GO enrichment analysis (C) and KEGG enrichment analysis (D) of KD-DEGs (DEGs in KD-MVIH group *vs*. KD-NC group); GO enrichment analysis (E) and KEGG enrichment analysis (F) of accordant DEGs. GO: Gene Ontology; KEGG: Kyoko Encyclopedia of Genes and Genomes; DEGs: differentially expressing genes; BP: biological processes; CC: cellular components; MF: molecular functions.

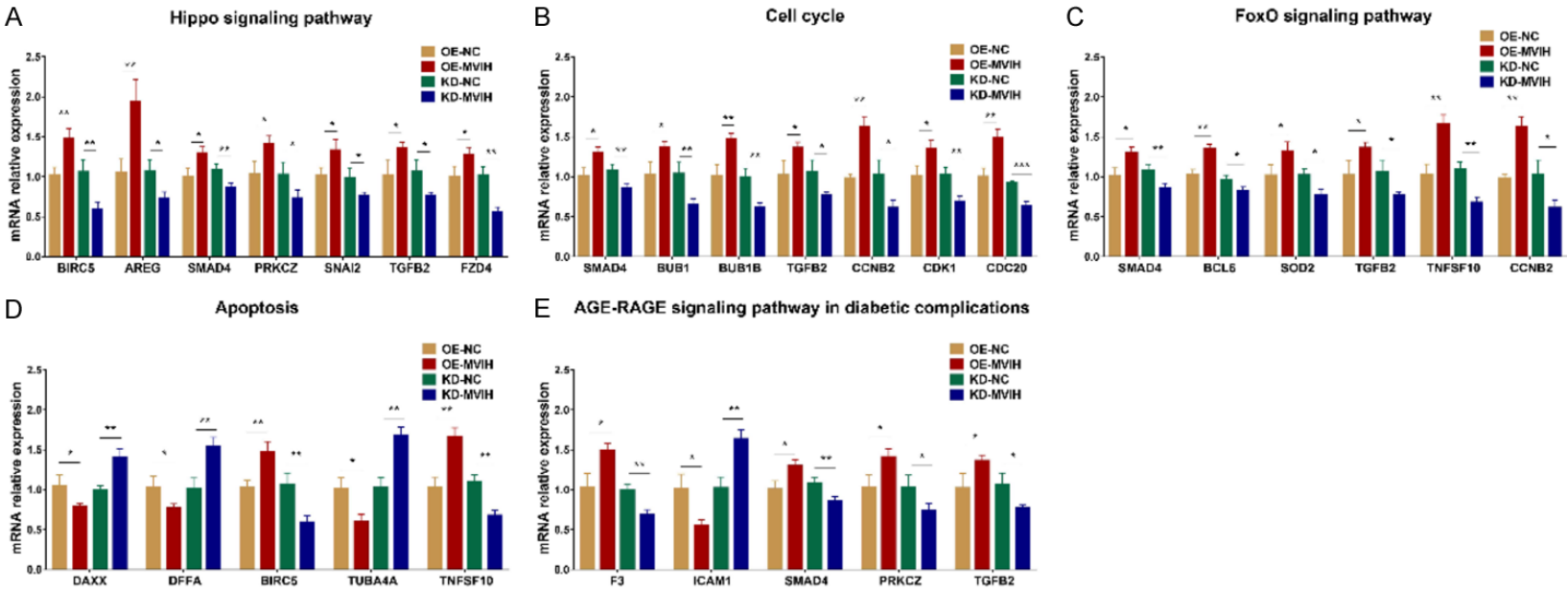

Figure 8. Validation for cancer-related pathways. The relative expressions of accordant DEGs implicated in Hippo signaling pathway (A), cell cycle (B), FoxO signaling pathway (C), apoptosis (D) and AGE-RAGE signaling pathway (E) in OE-MVIH group *vs.* OE-NC group and KD-MVIH group *vs.* KD-NC group. FoxO: Forkhead box O; AGE-RAGE signaling pathway: advanced glycation end products-RAGE signaling pathway; DEGs: differentially expressing genes.

Table 2. Patients' clinical characteristics

Items	PDAC Patients (N=70)
Age (years, M ± SD)	63.4±7.0
Male, No. (%)	41 (58.6)
History of smoke, No. (%)	39 (55.7)
History of drink, No. (%)	36 (51.4)
Tumor site, No. (%)	
Head	32 (45.7)
Body	25 (35.7)
Tail	13 (18.6)
Pathological grade, No. (%)	
G1	20 (28.6)
G2	20 (28.6)
G3	30 (42.8)
Tumor size (cm, M ± SD)	3.5±1.2
Lymph node metastasis, No. (%)	46 (65.7)
TNM Stage, No. (%)	
I	12 (17.1)
II	45 (64.3)
III	13 (18.6)

PDAC: Pancreatic Ductal Adenocarcinoma; M ± SD: mean ± standard deviation.

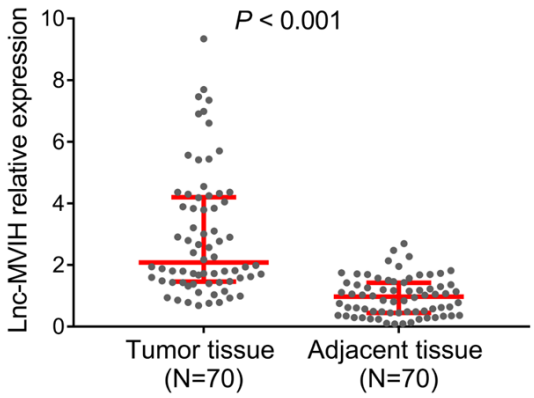

Figure 9. Lnc-MVIH expression was increased in tumor tissue compared to adjacent tissue in PDAC patients. Lnc-MVIH: long non-coding RNAs associated with microvascular invasion in hepatocellular carcinoma; PDAC: pancreatic ductal adenocarcinomas.

Lnc-MVIH expression in tumor tissue as well as adjacent tissue and its correlation with clinical characteristics

In vitro, we found that lnc-MVIH could regulate multiple cancer-related pathways to promote PDAC progression. Therefore, we further evaluated its clinical implication in PDAC monitoring and prognosis. We subsequently enrolled 70 PDAC patients underwent resection with the detailed clinical characteristics shown in **Table 2**. We also discovered that lnc-MVIH expression was increased in tumor tissue compared to adjacent tissue ($P<0.001$) (**Figure 9**). Based on the median value of tumor tissue lnc-MVIH expression, all PDAC patients were divided into lnc-MVIH high expression group and lnc-MVIH low expression group. Larger tumor size ($P=0.031$), lymph node metastasis ($P=0.012$) as well as higher TNM stage ($P=0.039$) were shown in lnc-MVIH high expression group compared to lnc-MVIH low expression group (**Table 3**). However, no difference was discovered between the two groups in other clinical characteristics including age ($P=0.454$), gender ($P=0.225$), history of smoke ($P=0.229$), history of drink ($P=1.000$), tumor site ($P=0.886$) and pathological grade ($P=0.333$) (**Table 3**).

Association of lnc-MVIH expression with OS

OS was worse in lnc-MVIH high expression group compared to lnc-MVIH low expression group (**Figure 10**). In addition, univariate Cox's regression showed that lnc-MVIH expression (high vs. low) ($P=0.011$) was correlated with shorter OS, and higher pathological grade ($P=0.010$), lymph node metastasis (yes vs. no) ($P=0.029$) and higher TNM stage ($P=0.001$) were correlated with poor OS in PDAC patients as well (**Table 4**). Further multivariate Cox's regression disclosed that lnc-MVIH expression (high vs. low) ($P=0.045$) could independently predict worse OS, and higher pathological grade ($P=0.024$) and higher TNM stage ($P=0.005$) were independent factors for predicting worse OS in PDAC patients as well.

Discussion

As a novelly identified lncRNA, lnc-MVIH (located within the intron of the encoding proteins for 40S ribosome (RPS) 24 gene) has been discovered as a tumor promoter in several carcinomas. For example, in non-small cell lung cancer (NSCLC), lnc-MVIH increases cell proliferation and accelerates cell invasion through upregulating matrix metalloproteinase (MMP) 2 and MMP9 protein expressions [10]. In breast cancer, upregulated lnc-MVIH expression enhances cell proliferation, suppresses apoptosis, decreases the percentage of cells in G1/G0 but increases those in the S phase, meanwhile, knockdown of lnc-MVIH shows the opposite trends [9]. In glioma, lnc-MVIH is upregulated in

Table 3. Correlation of lnc-MVIH with clinical characteristics

Items	Lnc-MVIH low, No. (%)	Lnc-MVIH high, No. (%)	*P* value
Age			0.454
≤60 years	11 (31.4)	14 (40.0)	
>60 years	24 (68.6)	21 (60.0)	
Gender			0.225
Male	18 (51.4)	23 (65.7)	
Female	17 (48.6)	12 (34.3)	
History of smoke			0.229
No	13 (37.1)	18 (51.4)	
Yes	22 (62.9)	17 (48.6)	
History of drink			1.000
No	17 (48.6)	17 (48.6)	
Yes	18 (51.4)	18 (51.4)	
Tumor site			0.886
Head	15 (42.9)	17 (48.6)	
Body	13 (37.1)	12 (34.3)	
Tail	7 (20.0)	6 (17.1)	
Pathological grade			0.333
G1	12 (34.3)	8 (22.9)	
G2	11 (31.4)	9 (25.7)	
G3	12 (34.3)	18 (51.4)	
Tumor size			0.031
≤2 cm	10 (28.6)	3 (8.6)	
>2 cm	25 (71.4)	32 (91.4)	
Lymph node metastasis			0.012
No	17 (48.6)	7 (20.0)	
Yes	18 (51.4)	28 (80.0)	
TNM Stage			0.039
I	10 (28.6)	2 (5.7)	
II	19 (54.3)	26 (74.3)	
III	6 (17.1)	7 (20.0)	

Comparison was determined by Chi-square test.

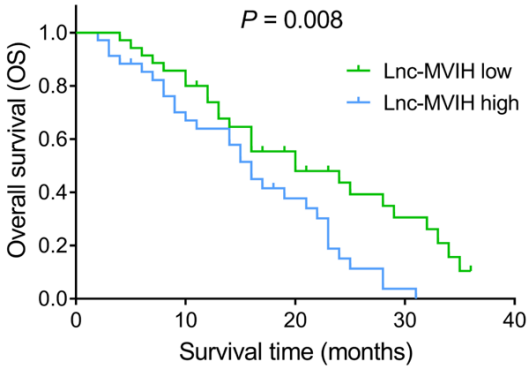

Figure 10. OS was worse in lnc-MVIH high expression group compared to lnc-MVIH low expression group in PDAC patients. Lnc-MVIH: long non-coding RNAs associated with microvascular invasion in hepatocellular carcinoma; OS: overall survival; PDAC: pancreatic ductal adenocarcinomas.

glioma cell lines, and its upregulation increases cell proliferation, invasion and migration, but its downregulation decreases proliferation, invasion and migration [17]. In HCC, lnc-MVIH not only represses miR-199a to accelerate cell growth and decrease cell apoptosis [11], but also interacts with AT-rich interactive domain-containing protein 1A (ARID1A) to promote cell proliferation and migration [18]. In addition, lnc-MVIH is also related to tumor angiogenesis. For instance, one previous study displays that lnc-MVIH induces angiogenesis via repressing the secretion of PGK1 to increase microvessel density, thereby accelerates tumor growth in HCC [7].

Considering the influence of lnc-MVIH on enhancing cell growth, migration, invasion, and activating tumor angiogenesis in various carcinomas, we hypothesized lnc-MVIH also had a carcinogenic influence on PDAC progression. Therefore, we detected lnc-MVIH expression *in vitro*, and discovered that lnc-MVIH expression was highly expressed in most human PDAC cell lines compared to human normal pancreatic ductal epithelial cell line, which was in line with previous studies about other cancers [7, 9-11]. Subsequently, we found that lnc-MVIH promoted cell proliferation, migration, invasion, but inhibited apoptosis in PDAC. The possible explanations were that (1) lnc-MVIH might regulate multiple cancer-related pathways in PDAC (such as Hippo signaling pathway, cell cycle-related pathway, FoxO signaling pathway, apoptosis-related pathway and AGE-RAGE signaling pathway) to increase cell proliferation, migration and invasion, thereby accelerated PDAC progression (which were discovered form the subsequent RNA sequencing). (2) lnc-MVIH, like its influence on NSCLC, might activate MMP2 and MMP9 to accelerate cell proliferation and invasion [10]. (3) lnc-MVIH, as in HCC, regulated several genes (including downregulating miR-199a or binding to ARID1A) to promote cell proliferation and migration, but inhibit cell apoptosis [11, 18]. (4) lnc-MVIH, just as its influence on tumor angiogenesis of HCC, decreased the secretion of PGK1 to enhance microvessel den-

Table 4. Predictors for OS

Items	Univariate Cox's regression		Multivariate Cox's regression	
	P value	HR (95% CI)	*P* value	HR (95% CI)
Lnc-MVIH (high vs. low)	0.011	2.086 (1.180-3.689)	0.045	1.941 (1.014-3.716)
Age (>60 vs. ≤60 years)	0.791	0.928 (0.532-1.616)	0.869	0.950 (0.514-1.754)
Gender (male vs. female)	0.852	0.950 (0.554-1.630)	0.385	0.748 (0.388-1.441)
History of smoke (yes vs. no)	0.623	0.875 (0.513-1.491)	0.690	0.867 (0.431-1.747)
History of drink (yes vs. no)	0.717	1.105 (0.645-1.893)	0.719	1.125 (0.592-2.137)
Tumor site				
Tail		Reference		Reference
Head	0.907	1.046 (0.494-2.213)	1.000	1.000 (0.449-2.228)
Body	0.379	1.399 (0.662-2.955)	0.909	1.047 (0.476-2.304)
Higher pathological grade	0.010	1.570 (1.115-2.213)	0.024	1.581 (1.062-2.353)
Tumor size (>2 vs. ≤2 cm)	0.097	2.052 (0.878-4.798)	0.846	0.907 (0.338-2.432)
Lymph node metastasis (yes vs. no)	0.029	1.970 (1.070-3.625)	0.731	0.881 (0.426-1.819)
Higher TNM Stage	0.001	2.199 (1.376-3.513)	0.005	2.351 (1.291-4.282)

OS, overall survival; HR, hazard ratio; CI, confidence interval.

sity and accelerate angiogenesis, subsequently contributing to tumor growth [7].

In order to investigate the comprehensively molecular mechanism of lnc-MVIH in PDAC pathogenesis, we further performed RNA sequencing and bioinformatics in lnc-MVIH dysregulated and control PDAC cells. A total of 196 accordant DEGs (including 145 DEGs upregulated in OE-MVIH group *vs.* OE-NC group and downregulated in KD-MVIH group *vs.* KD-NC group, and 51 DEGs downregulated in OE-MVIH group *vs.* OE-NC group and upregulated in KD-MVIH group *vs.* KD-NC group) were observed. In addition, GO enrichment analysis disclosed that they were enriched in several cancer-related biological processes (such as positive regulation of proliferation, positive regulation of cell migration and regulation of cell cycle). Furthermore, KEGG enrichment analysis showed that these DEGs were enriched in multiple cancer-related pathways (such as Hippo signaling pathway, cell cycle-related pathway, FoxO signaling pathway, apoptosis-related pathway and AGE-RAGE signaling pathway). Among these pathways, (1) Hippo signaling pathway is a highly conserved pathway and participants in tumorigenesis, stem cell self-renewal and differentiation as well as organ size control [19]. (2) Cell cycle-related pathways directly influences cell growth to affect tumor progression. (3) FoxO signaling pathway usually interacts with phosphatidylinositol 3-kinase (PI3K)/protein kinase (AKT) pathway to induce tumor formation and growth in several cancers [20, 21]. (4) Apoptosis-related pathways directly impacts cancer cell apoptosis to influence tumor growth. (5) AGE-RAGE signaling pathway increases ERK phosphorylation, MMP2, and MMP9 to accelerate cell proliferation and migration in various cancers (including oral cancer and prostate cancer) [22, 23]. Subsequently, we further validated the relative expressions of accordant DEGs implicated in above-mentioned 5 cancer-related pathways through RT-qPCR, and found that most of these accordant DEGs were mediated by lnc-MVIH in PDAC cells. These observations suggested that lnc-MVIH could regulate multiple cancer-related pathways to accelerate PDAC progression, which supplied deeper and more comprehensive insights for the molecular mechanisms of lnc-MVIH in PDAC pathology. However, in this study, we used mRNA sequencing and bioinformatics to determine the downstream pathways of lnc-MVIH, hence, RT-qPCR was the most direct method for validation of mRNA expressions. As to protein, it was preferred to perform Western Blot for further validation of pathways regulated by lnc-MVIH. Therefore, further validation is needed. Furthermore, the detailed mechanism of lnc-MVIH regulating these 5 cancer-related pathways in PDAC is still unclear, further study is necessary.

Clinically, several studies have been performed to explore the clinical implication of lnc-MVIH in cancer patients, and disclose that lnc-MVIH high expression has a positive relationship with lymph node metastasis and advanced clinical

stage in cancer patients (including HCC, NSCLC and gastric cancer) [9, 10, 24]. However, there is still limited information about the role of lnc-MVIH in PDAC. Based on the above-mentioned *in vitro* results about lnc-MVIH was a tumor promoter in PDAC, we further evaluated its clinical implication in PDAC monitoring and prognosis, and discovered the positive correlation of lnc-MVIH expression with tumor size, lymph node metastasis and TNM stage in PDAC patients, which might be due to that (1) lnc-MVIH activated several oncogenic pathways (Hippo signaling pathway, FoxO signaling pathway and AGE-RAGE signaling pathway and so on) to promote PDAC progression, thereby caused aggravated disease conditions in PDAC patients (as shown by the above-mentioned results). (2) lnc-MVIH increased cell growth via regulating multiple cancer-related pathways (cell cycle-related pathways and apoptosis-related pathways et.al), and subsequently led to tumor growth and ultimately contributed to disease exacerbation in PDAC patients (which were shown in the above-mentioned results). (3) lnc-MVIH regulated multiple genes, including activating MMP2 and MMP9 (just like its influence on NSCLC [10]), downregulating miR-199a (just like its function on HCC [11]) or binding to ARID1A (just like its function on HCC [18]) to promote cell proliferation and migration, but inhibited apoptosis, which subsequently accelerated tumor growth and tumor metastasis in PDAC patients. For the influence of lnc-MVIH on prognosis in cancer patients, several previous studies reveal that lnc-MVIH is related to poor relapse free survival (RFS) in NSCLC patients [10], shorter OS as well as disease-free survival (DFS) in breast cancer patients [9]; shorter OS in glioma patients [17]. Taken together, lnc-MVIH works as a predictive factor for worse prognosis in several cancer patients. In accordance with these previous data, we also found that lnc-MVIH acted as an independent factor predicting worse OS in PDAC patients, which might be caused by that: (1) lnc-MVIH was related to aggravated disease conditions, thereby led to poor prognosis in PDAC patients. (2) lnc-MVIH might increase drug resistance and postoperative recurrence by activating several pathways (such as Hippo signaling pathway and FoxO signaling pathway), resulting in worse prognosis in PDAC patients [19, 20]. In brief, these data indicated that lnc-MVIH played as a tumor promoter in PDAC progression and acted as an independent factor predicting poor prognosis in PDAC patients. However, the sample size in this study was relatively small, which might cause poor statistical power, further validation in a larger population is needed.

In conclusion, lnc-MVIH promoted PDAC cell proliferation, migration, invasion via regulating multiple cancer-related pathways (Hippo signaling pathway, cell cycle-related pathways, FoxO signaling pathway, apoptosis-related pathways as well as AGE-RAGE signaling pathway et al.), and correlated with aggravated clinical features as well as poor prognosis in PDAC patients, which indicated that lnc-MVIH might be a potential therapeutic target in PDAC.

Acknowledgements

This work was supported by the Natural Science Foundation of China (No. 81873529), Natural Science Foundation of Hubei province (No. 2019CFB729) and Research foundation of Union hospital (No. 4827).

Disclosure of conflict of interest

None.

Address correspondence to: Wei Zhou, Department of Pancreatic Surgery, Union Hospital, Tongji Medical College, Huazhong University of Science and Technology, 1277 Jiefang Avenue, Wuhan 430022, Hubei Province, China. Tel: +86-027-85351631; E-mail: PDIZhou@hust.edu.cn; Weici Wang, Department of Vascular Surgery, Union Hospital, Tongji Medical College, Huazhong University of Science and Technology, 1277 Jiefang Avenue, Wuhan 430022, Hubei Province, China. Tel: +86-18071705166; E-mail: 4121385@qq.com

References

[1] Adamska A, Domenichini A and Falasca M. Pancreatic ductal adenocarcinoma: current and evolving therapies. Int J Mol Sci 2017; 18.

[2] Rahib L, Smith BD, Aizenberg R, Rosenzweig AB, Fleshman JM and Matrisian LM. Projecting cancer incidence and deaths to 2030: the unexpected burden of thyroid, liver, and pancreas cancers in the United States. Cancer Res 2014; 74: 2913-2921.

[3] Hwang CI, Boj SF, Clevers H and Tuveson DA. Preclinical models of pancreatic ductal adenocarcinoma. J Pathol 2016; 238: 197-204.

[4] Munoz Martin AJ, Adeva J, Martinez-Galan J, Reina JJ and Hidalgo M. Pancreatic ductal adenocarcinoma: metastatic disease. Clin Transl Oncol 2017; 19: 1423-1429.

[5] Kumar MM and Goyal R. LncRNA as a therapeutic target for angiogenesis. Curr Top Med Chem 2017; 17: 1750-1757.
[6] Wapinski O and Chang HY. Long noncoding RNAs and human disease. Trends Cell Biol 2011; 21: 354-361.
[7] He Y, Meng XM, Huang C, Wu BM, Zhang L, Lv XW and Li J. Long noncoding RNAs: novel insights into hepatocelluar carcinoma. Cancer Lett 2014; 344: 20-27.
[8] Yuan SX, Yang F, Yang Y, Tao QF, Zhang J, Huang G, Yang Y, Wang RY, Yang S, Huo XS, Zhang L, Wang F, Sun SH and Zhou WP. Long noncoding RNA associated with microvascular invasion in hepatocellular carcinoma promotes angiogenesis and serves as a predictor for hepatocellular carcinoma patients' poor recurrence-free survival after hepatectomy. Hepatology 2012; 56: 2231-2241.
[9] Lei B, Xu SP, Liang XS, Li YW, Zhang JF, Zhang GQ and Pang D. Long non-coding RNA MVIH is associated with poor prognosis and malignant biological behavior in breast cancer. Tumour Biol 2016; 37: 5257-5264.
[10] Nie FQ, Zhu Q, Xu TP, Zou YF, Xie M, Sun M, Xia R and Lu KH. Long non-coding RNA MVIH indicates a poor prognosis for non-small cell lung cancer and promotes cell proliferation and invasion. Tumour Biol 2014; 35: 7587-7594.
[11] Shi Y, Song Q, Yu S, Hu D and Zhuang X. Microvascular invasion in hepatocellular carcinoma overexpression promotes cell proliferation and inhibits cell apoptosis of hepatocellular carcinoma via inhibiting miR-199a expression. Onco Targets Ther 2015; 8: 2303-2310.
[12] Zhang ZL, Bai ZH, Wang XB, Bai L, Miao F and Pei HH. miR-186 and 326 predict the prognosis of pancreatic ductal adenocarcinoma and affect the proliferation and migration of cancer cells. PLoS One 2015; 10: e0118814.
[13] Head SR, Komori HK, LaMere SA, Whisenant T, Van Nieuwerburgh F, Salomon DR and Ordoukhanian P. Library construction for next-generation sequencing: overviews and challenges. Biotechniques 2014; 56: 61-64, 66, 68, passim.
[14] Trapnell C, Pachter L and Salzberg SL. TopHat: discovering splice junctions with RNA-Seq. Bioinformatics 2009; 25: 1105-1111.
[15] Love MI, Huber W and Anders S. Moderated estimation of fold change and dispersion for RNA-seq data with DESeq2. Genome Biol 2014; 15: 550.
[16] Huang DW, Sherman BT, Tan Q, Kir J, Liu D, Bryant D, Guo Y, Stephens R, Baseler MW, Lane HC and Lempicki RA. DAVID bioinformatics resources: expanded annotation database and novel algorithms to better extract biology from large gene lists. Nucleic Acids Res 2007; 35: W169-175.
[17] Zhuang JJ, Yue M, Zheng YH, Li JP and Dong XY. Long non-coding RNA MVIH acts as a prognostic marker in glioma and its role in cell migration and invasion. Eur Rev Med Pharmacol Sci 2016; 20: 4898-4904.
[18] Cheng S, Wang L, Deng CH, Du SC and Han ZG. ARID1A represses hepatocellular carcinoma cell proliferation and migration through lncRNA MVIH. Biochem Biophys Res Commun 2017; 491: 178-182.
[19] Tao Y, Cai F, Shan L, Jiang H, Ma L and Yu Y. The Hippo signaling pathway: an emerging anticancer drug target. Discov Med 2017; 24: 7-18.
[20] Farhan M, Wang H, Gaur U, Little PJ, Xu J and Zheng W. FOXO signaling pathways as therapeutic targets in cancer. Int J Biol Sci 2017; 13: 815-827.
[21] Mei Q, Li X, Zhang K, Wu Z, Li X, Meng Y, Guo M, Luo G, Fu X and Han W. Genetic and methylation-induced loss of miR-181a2/181b2 within chr9q33.3 facilitates tumor growth of cervical cancer through the PIK3R3/Akt/FoxO signaling pathway. Clin Cancer Res 2017; 23: 575-586.
[22] Ko SY, Ko HA, Shieh TM, Chang WC, Chen HI, Chang SS and Lin IH. Cell migration is regulated by AGE-RAGE interaction in human oral cancer cells in vitro. PLoS One 2014; 9: e110542.
[23] Bao JM, He MY, Liu YW, Lu YJ, Hong YQ, Luo HH, Ren ZL, Zhao SC and Jiang Y. AGE/RAGE/Akt pathway contributes to prostate cancer cell proliferation by promoting Rb phosphorylation and degradation. Am J Cancer Res 2015; 5: 1741-1750.
[24] Zhang Y, Lin S, Yang X and Zhang X. Prognostic and clinicopathological significance of lncRNA MVIH in cancer patients. J Cancer 2019; 10: 1503-1510.

Supplementary Table 1. Primers

Gene	Forward Primer (5'-3')	Reverse Primer (5'-3')
Lnc-MVIH	AATTTTGCACATCTGAACAGCC	TTCAAAATCCCACTACGCCCA
BIRC5	GACCACCGCATCTCTACATTCA	CAAGTCTGGCTCGTTCTCAGT
AREG	GTGGTGCTGTCGCTCTTGA	TGTGGTTCGTTATCATACTCTTCTG
SMAD4	GCCATCGTTGTCCACTGAAGG	AATCCATTCTGCTGCTGTCCTG
PRKCZ	CCTGGTGCGGTTGAAGAAGAAT	GTAGAACCTGGCGTGCTCCT
SNAI2	TTCGGACCCACACATTACCTTG	CACAGCAGCCAGATTCCTCAT
TGFB2	AGAGTGCCTGAACAACGGATT	GCCATTCGCCTTCTGCTCTT
FZD4	CACAGAACGACCACAACCACAT	AGCCAGCATCATAGCCACACT
BUB1	GCTGGCTTGGCACTGATTGA	GGCTTACACTCTCCTCCTTCATT
BUB1B	CTCTGGCTTCTCTGGTTCTTCTG	AACTTAGGCATTGGTCTGTCTTCT
CCNB2	GCTGCTTCCTGCTTGTCTCA	GCATACTTATTCTTGATGGCGATGA
CDK1	CAGTCTTCAGGATGTGCTTATGC	TGTACTGACCAGGAGGGATAGAAT
CDC20	GCAGACATTCACCCAGCATCA	CATCCACGGCACTCAGACAG
BCL6	TCGTGAGGTGGTGGAGAACAA	GAGAAGAGGAGGCTGCTGACA
SOD2	GCCCTGGAACCTCACATCAAC	CAACGCCTCCTGGTACTTCTC
TNFSF10	GTCAAGTGGCAACTCCGTCAG	GACCAGTTCACCATTCCTCAAGT
DAXX	ACGATGAGGAGAGTGATGAGGA	TTACCTGCTGCTGCTTCTTCC
DFFA	TGTCCAGCATCATCCTCCTATCA	CCTCCTGAACAGTCTCCGTCTT
TUBA4A	CGACTCCTTCACCACCTTCTTC	ATAGTTGTTGGCAGCATCCTCTT
F3	AAGTGAATGTGACCGTAGAAGATGA	GCCAGGATGATGACAAGGATGAT
ICAM1	CCTATGGCAACGACTCCTTCTC	TGTCTCCTGGCTCTGGTTCC
GAPDH	GACCACAGTCCATGCCATCAC	ACGCCTGCTTCACCACCTT

Supplementary Table 2. 196 accordant DEGs by RNA-sequencing

Gene ID	Symbol	OE log_2FC	OE *P* value	OE P_{adj} value	KD log_2FC	KD *P* value	KD P_{adj} value	OE Trend	KD Trend
ENSG00000109321	AREG	-5.517902831	6.23809E-05	0.001703175	5.029854373	0.000143272	0.001595989	DOWN	UP
ENSG00000105509	HAS1	-4.149634516	2.89291E-07	2.66574E-05	4.512561629	2.02419E-08	9.90902E-07	DOWN	UP
ENSG00000109511	ANXA10	-2.782527805	1.38844E-05	0.000533739	3.766390009	4.50961E-08	1.98296E-06	DOWN	UP
ENSG00000181195	PENK	-3.043536373	3.79816E-07	3.21612E-05	2.945184575	7.05511E-07	1.92206E-05	DOWN	UP
ENSG00000115155	OTOF	-2.890112065	0.002936197	0.027460018	2.744215369	0.001874643	0.012472997	DOWN	UP
ENSG00000172201	ID4	-3.00115861	0.000107282	0.00253192	2.591322441	4.11643E-05	0.000582905	DOWN	UP
ENSG00000104435	STMN2	-3.689883671	7.22813E-08	8.31036E-06	1.875074251	0.005059039	0.025657581	DOWN	UP
ENSG00000112541	PDE10A	-1.580328223	0.006308047	0.046528811	3.687305188	5.2084E-09	2.99411E-07	DOWN	UP
ENSG00000117318	ID3	-1.902378511	0.00502972	0.039793211	3.351029598	8.52861E-07	2.25963E-05	DOWN	UP
ENSG00000170577	SIX2	-2.805344061	5.98246E-06	0.000271638	2.398051022	0.000115073	0.001335724	DOWN	UP
ENSG00000095752	IL11	-2.400449419	4.27725E-05	0.001291628	2.506194037	4.40951E-06	8.89855E-05	DOWN	UP
ENSG00000187134	AKR1C1	-1.940651041	5.52141E-05	0.001554927	2.917390832	1.36062E-09	1.02103E-07	DOWN	UP
ENSG00000174600	CMKLR1	-2.63417249	4.65123E-05	0.001383574	2.110669381	0.001163359	0.008564871	DOWN	UP
ENSG00000157193	LRP8	-2.260532264	2.84357E-09	5.74769E-07	2.466297081	7.39334E-11	8.644E-09	DOWN	UP
ENSG00000112319	EYA4	-2.33966634	5.38254E-05	0.001533044	2.301787771	7.44854E-05	0.0009372	DOWN	UP
ENSG00000127824	TUBA4A	-1.94751913	8.38793E-07	5.93884E-05	2.543843416	1.39244E-10	1.50432E-08	DOWN	UP
ENSG00000176697	BDNF	-2.525015449	0.000171652	0.003532257	1.841177523	0.005846846	0.028444362	DOWN	UP
ENSG00000102760	RGCC	-2.447497774	1.77044E-07	1.74702E-05	1.900973331	1.83558E-05	0.000291922	DOWN	UP
ENSG00000142178	SIK1	-1.829351086	0.00177235	0.019032637	2.332570101	3.76799E-05	0.00054028	DOWN	UP
ENSG00000149485	FADS1	-1.473720172	0.003146754	0.028913938	2.562691978	2.83037E-07	9.02548E-06	DOWN	UP
ENSG00000049192	ADAMTS6	-2.884278776	1.32812E-11	6.93498E-09	1.149211023	0.006466783	0.03075306	DOWN	UP
ENSG00000109819	PPARGC1A	-2.135442647	0.003103439	0.028597273	1.885027169	0.009688134	0.04118443	DOWN	UP
ENSG00000164112	TMEM155	-1.71379767	0.00487494	0.038964611	2.241376116	0.000296735	0.00284521	DOWN	UP
ENSG00000117525	F3	-1.494140795	3.78664E-05	0.001170946	2.449837335	1.54975E-11	2.24897E-09	DOWN	UP
ENSG00000144655	CSRNP1	-1.352652223	0.005024237	0.039774946	2.165256154	4.63864E-06	9.28616E-05	DOWN	UP
ENSG00000065320	NTN1	-1.786937497	0.004728758	0.038381347	1.712250925	0.006486816	0.030824982	DOWN	UP
ENSG00000154127	UBASH3B	-1.674337462	9.34059E-05	0.00229073	1.712825545	6.19874E-05	0.000815994	DOWN	UP
ENSG00000169933	FRMPD4	-2.215493313	6.11063E-10	1.53157E-07	1.138046921	0.000881811	0.006796345	DOWN	UP
ENSG00000174804	FZD4	-1.424323734	0.004385755	0.036641523	1.731977921	0.000543604	0.004628019	DOWN	UP
ENSG00000163132	MSX1	-1.465561839	4.96279E-08	5.98017E-06	1.637569652	9.69319E-10	7.69868E-08	DOWN	UP
ENSG00000138311	ZNF365	-1.300272252	0.001080587	0.013160273	1.780886476	4.70414E-06	9.35751E-05	DOWN	UP
ENSG00000198805	PNP	-1.56055547	0.000465426	0.007355253	1.476776594	0.000831176	0.00649395	DOWN	UP
ENSG00000164220	F2RL2	-1.809671977	1.30633E-08	2.06617E-06	1.159853711	0.000281115	0.002724619	DOWN	UP
ENSG00000254726	MEX3A	-1.030982092	0.001775512	0.019033979	1.849354719	2.42228E-08	1.14763E-06	DOWN	UP

ENSG00000102393	GLA	-1.118591103	0.000811468	0.010758051	1.7133687	3.0919E-07	9.70133E-06	DOWN	UP
ENSG00000179242	CDH4	-1.460809473	0.004893393	0.039035013	1.305002121	0.00862491	0.037766378	DOWN	UP
ENSG00000019549	SNAI2	-1.357405954	0.001670937	0.018193029	1.37955936	0.001404013	0.009940727	DOWN	UP
ENSG00000111802	TDP2	-1.187429223	5.61652E-10	1.43645E-07	1.526127148	1.97575E-15	1.37556E-12	DOWN	UP
ENSG00000142657	PGD	-1.042564946	0.000645569	0.009270172	1.661835746	5.44614E-08	2.29801E-06	DOWN	UP
ENSG00000163710	PCOLCE2	-1.459794888	1.27465E-06	8.31973E-05	1.244554585	3.63543E-05	0.000523898	DOWN	UP
ENSG00000132429	POPDC3	-1.545971498	9.97691E-10	2.31538E-07	1.031027254	4.53113E-05	0.00063517	DOWN	UP
ENSG00000213694	S1PR3	-1.169888979	0.000217707	0.004197387	1.262962781	6.83098E-05	0.000883445	DOWN	UP
ENSG00000176853	FAM91A1	-1.281512282	1.43831E-05	0.000544313	1.14675562	0.000103433	0.001234501	DOWN	UP
ENSG00000123505	AMD1	-1.357147278	1.54437E-05	0.000577734	1.067045451	0.000676932	0.005541313	DOWN	UP
ENSG00000181751	C5orf30	-1.317809168	4.39445E-15	7.86731E-12	1.068076947	1.61466E-10	1.70041E-08	DOWN	UP
ENSG00000154511	FAM69A	-1.177367189	0.004105796	0.035033269	1.165099234	0.004588006	0.023739427	DOWN	UP
ENSG00000084710	EFR3B	-1.044119039	0.000629231	0.009169216	1.280137848	2.21797E-05	0.000346148	DOWN	UP
ENSG00000140945	CDH13	-1.113777577	0.00622464	0.046158227	1.203719402	0.003065765	0.017607774	DOWN	UP
ENSG00000143819	EPHX1	-1.181412667	0.004261998	0.03592256	1.130901606	0.006248654	0.029900748	DOWN	UP
ENSG00000080824	HSP90AA1	-1.061319094	0.00654009	0.047596056	1.120014151	0.00410563	0.02188505	DOWN	UP
ENSG00000128805	ARHGAP22	-1.084848212	0.006830384	0.048885422	1.05835905	0.008128572	0.036174454	DOWN	UP
ENSG00000010932	FMO1	5.225165157	2.0915E-12	1.54181E-09	-4.544621629	1.21659E-07	4.45036E-06	UP	DOWN
ENSG00000116455	WDR77	5.26390779	7.81391E-12	4.8962E-09	-3.861379949	3.47226E-07	1.06357E-05	UP	DOWN
ENSG00000157368	IL34	4.570328715	3.45341E-11	1.39607E-08	-4.434614607	5.34914E-10	4.82269E-08	UP	DOWN
ENSG00000135451	TROAP	4.781395878	4.25036E-06	0.000210015	-3.676758466	2.87662E-05	0.000433812	UP	DOWN
ENSG00000121858	TNFSF10	3.365465841	1.02842E-06	7.00445E-05	-4.951664115	6.52269E-12	1.13531E-09	UP	DOWN
ENSG00000213699	SLC35F6	2.982102636	0.001045349	0.01285605	-5.196896788	7.52597E-09	4.17325E-07	UP	DOWN
ENSG00000129195	FAM64A	3.723916019	1.04359E-05	0.000423247	-4.358247492	2.57851E-08	1.21026E-06	UP	DOWN
ENSG00000198171	DDRGK1	3.204350523	0.000453469	0.007220931	-4.605853093	1.84689E-07	6.30661E-06	UP	DOWN
ENSG00000188257	PLA2G2A	4.118371103	1.46386E-09	3.16295E-07	-3.626567472	3.00188E-07	9.47541E-06	UP	DOWN
ENSG00000117650	NEK2	3.022067345	0.000461543	0.007307291	-4.712968478	1.64367E-08	8.20657E-07	UP	DOWN
ENSG00000090339	ICAM1	4.581841772	2.71423E-08	3.61859E-06	-3.01359704	0.000255278	0.002534979	UP	DOWN
ENSG00000089685	BIRC5	3.186650835	4.77544E-05	0.001404831	-4.366170752	7.86254E-09	4.28406E-07	UP	DOWN
ENSG00000214357	NEURL1B	2.770745092	0.000785218	0.010501983	-4.440696017	2.08829E-08	1.01602E-06	UP	DOWN
ENSG00000075218	GTSE1	2.844529673	0.000133367	0.002951981	-4.356057501	3.11885E-09	1.99415E-07	UP	DOWN
ENSG00000172348	RCAN2	2.798048973	9.86353E-06	0.000405278	-4.313400423	8.42645E-12	1.37143E-09	UP	DOWN
ENSG00000157456	CCNB2	3.094194603	3.61525E-06	0.000187993	-3.831455259	3.27641E-09	2.07373E-07	UP	DOWN
ENSG00000115163	CENPA	3.434455069	0.000212996	0.004131995	-3.443628991	6.69303E-05	0.000870997	UP	DOWN
ENSG00000138180	CEP55	2.69770171	0.000146449	0.003164312	-3.776562044	5.2634E-08	2.23596E-06	UP	DOWN
ENSG00000011426	ANLN	2.108293616	0.000224631	0.004299703	-4.182853623	1.93917E-13	5.65154E-11	UP	DOWN

ENSG00000166803	KIAA0101	2.306834269	0.002457252	0.023983085	-3.92678668	2.1053E-07	7.01693E-06	UP	DOWN
ENSG00000169679	BUB1	2.38394042	0.00076589	0.010342821	-3.821648017	4.88892E-08	2.09822E-06	UP	DOWN
ENSG00000090889	KIF4A	2.586192248	4.50294E-05	0.001343593	-3.60354046	4.0187E-09	2.44794E-07	UP	DOWN
ENSG00000125730	C3	3.478630713	0.00070411	0.009806163	-2.703365021	0.008466256	0.037297124	UP	DOWN
ENSG00000117399	CDC20	2.328786691	0.004106597	0.035033269	-3.80011901	2.18749E-06	5.03002E-05	UP	DOWN
ENSG00000156970	BUB1B	2.121879536	0.001497042	0.016916976	-3.98846789	1.66357E-09	1.1843E-07	UP	DOWN
ENSG00000008517	IL32	3.414142554	3.52151E-07	3.08613E-05	-2.613987844	5.68573E-05	0.00076207	UP	DOWN
ENSG00000186185	KIF18B	1.970639926	0.005974256	0.044778338	-3.879020953	2.64134E-08	1.23512E-06	UP	DOWN
ENSG00000243649	CFB	3.239149754	0.000104822	0.002503446	-2.604181948	0.001811475	0.012120346	UP	DOWN
ENSG00000172901	LVRN	2.436220932	1.06656E-11	6.36479E-09	-3.374654287	5.78287E-20	8.05233E-17	UP	DOWN
ENSG00000178999	AURKB	1.972760463	0.001170454	0.013982959	-3.730359522	7.48255E-11	8.644E-09	UP	DOWN
ENSG00000167900	TK1	2.045878024	0.003625784	0.032120047	-3.617351062	2.32382E-07	7.64358E-06	UP	DOWN
ENSG00000170312	CDK1	2.051335906	0.002076519	0.021260567	-3.556125255	7.39408E-08	2.94167E-06	UP	DOWN
ENSG00000179348	GATA2	2.119424632	0.000560186	0.008499091	-3.484934745	9.00888E-09	4.80422E-07	UP	DOWN
ENSG00000113070	HBEGF	2.92448692	1.03166E-07	1.1341E-05	-2.642315369	1.84329E-06	4.33398E-05	UP	DOWN
ENSG00000154839	SKA1	1.976029342	0.002587726	0.025003381	-3.580128056	1.15776E-08	5.97083E-07	UP	DOWN
ENSG00000244731	C4A	3.983851348	1.44157E-13	1.80657E-10	-1.571011886	0.003837479	0.020918352	UP	DOWN
ENSG00000123700	KCNJ2	3.096127542	3.73229E-06	0.000192482	-2.391972423	0.000545729	0.004642961	UP	DOWN
ENSG00000198959	TGM2	2.534652425	3.62505E-09	7.0983E-07	-2.891760187	1.86395E-11	2.53902E-09	UP	DOWN
ENSG00000224389	C4B	3.720515812	1.92341E-12	1.52484E-09	-1.613713616	0.002837202	0.016591606	UP	DOWN
ENSG00000198901	PRC1	2.156917155	3.89398E-05	0.001199002	-3.1445939	1.16363E-09	8.83793E-08	UP	DOWN
ENSG00000167508	MVD	2.257367239	4.74472E-05	0.001399389	-3.02394692	8.34598E-08	3.27874E-06	UP	DOWN
ENSG00000149633	KIAA1755	3.09151426	9.7764E-07	6.69497E-05	-2.025666861	0.001454904	0.010230685	UP	DOWN
ENSG00000163347	CLDN1	2.720413003	0.003447391	0.030903218	-2.382333384	0.005292581	0.02646713	UP	DOWN
ENSG00000104147	OIP5	1.959215374	0.003943529	0.034153636	-3.134398657	1.79338E-06	4.2405E-05	UP	DOWN
ENSG00000163808	KIF15	1.484605923	0.006073681	0.045387818	-3.581951512	2.26977E-11	3.05858E-09	UP	DOWN
ENSG00000142583	SLC2A5	2.721625042	7.99214E-06	0.000343005	-2.335001409	0.000139798	0.001569851	UP	DOWN
ENSG00000014123	UFL1	2.744574656	5.69937E-09	1.03514E-06	-2.239837259	7.46108E-06	0.000136699	UP	DOWN
ENSG00000136514	RTP4	2.6075735	1.27755E-09	2.80881E-07	-2.340136528	9.90547E-08	3.81955E-06	UP	DOWN
ENSG00000169245	CXCL10	1.367810246	0.000705162	0.009808097	-3.512251942	3.91535E-19	4.08893E-16	UP	DOWN
ENSG00000035664	DAPK2	2.718671054	5.00261E-09	9.49889E-07	-2.154658706	1.74758E-06	4.15214E-05	UP	DOWN
ENSG00000065883	CDK13	2.672483661	5.26189E-07	4.09578E-05	-2.16697678	5.83342E-05	0.000780197	UP	DOWN
ENSG00000067606	PRKCZ	3.104250069	1.09244E-07	1.19048E-05	-1.718991455	0.004415878	0.023058242	UP	DOWN
ENSG00000173114	LRRN3	2.167795038	0.000153116	0.0032857	-2.607293462	5.89874E-06	0.00011286	UP	DOWN
ENSG00000068489	PRR11	1.686599492	4.09135E-05	0.001241471	-3.063630485	1.66848E-14	6.74498E-12	UP	DOWN
ENSG00000016402	IL2ORA	2.680446132	0.00021083	0.004096309	-2.067646532	0.004744543	0.02440605	UP	DOWN

ENSG00000005471	ABCB4	2.882688324	5.76262E-07	4.40348E-05	-1.839347422	0.003991426	0.021513903	UP	DOWN
ENSG00000137573	SULF1	2.87039883	1.85995E-06	0.000115004	-1.850901625	0.002168021	0.013847931	UP	DOWN
ENSG00000254087	LYN	2.722799363	1.17622E-07	1.25986E-05	-1.979015176	0.000118518	0.001366287	UP	DOWN
ENSG00000076382	SPAG5	1.737911118	0.000157228	0.003323543	-2.954977665	4.84281E-11	6.13031E-09	UP	DOWN
ENSG00000144596	GRIP2	2.280518673	0.000697244	0.00976297	-2.350139883	0.000463642	0.004066031	UP	DOWN
ENSG00000100100	PIK3IP1	1.498808819	0.002308876	0.023110889	-3.125352615	4.11617E-10	3.84954E-08	UP	DOWN
ENSG00000112096	SOD2	2.275075405	0.004647894	0.038020504	-2.28896404	0.004403699	0.023042653	UP	DOWN
ENSG00000124212	PTGIS	2.544983135	6.78691E-06	0.000302682	-1.974281896	0.000483832	0.004212309	UP	DOWN
ENSG00000138642	HERC6	1.837857566	0.001493701	0.016909318	-2.668825316	3.79015E-06	7.78658E-05	UP	DOWN
ENSG00000168078	PBK	1.801026374	0.003202472	0.029315833	-2.695437797	6.721E-06	0.000126089	UP	DOWN
ENSG00000102524	TNFSF13B	2.709895571	1.04115E-05	0.000423247	-1.769902152	0.003993085	0.021513903	UP	DOWN
ENSG00000131979	GCH1	2.352158406	1.68118E-05	0.000619662	-2.090950569	0.00013112	0.001491103	UP	DOWN
ENSG00000013810	TACC3	1.370177672	0.001225064	0.014497165	-3.048462238	3.95631E-13	1.03293E-10	UP	DOWN
ENSG00000118257	NRP2	1.667677172	6.42058E-05	0.001745394	-2.708065254	8.30785E-11	9.29589E-09	UP	DOWN
ENSG00000069535	MAOB	2.71940512	5.52628E-06	0.000258415	-1.617247961	0.008055766	0.03591985	UP	DOWN
ENSG00000065534	MYLK	1.730153162	1.90209E-05	0.000671464	-2.379433172	4.12237E-09	2.46707E-07	UP	DOWN
ENSG00000188112	C6orf132	1.642627886	2.59669E-06	0.000147248	-2.440207577	9.27782E-12	1.47177E-09	UP	DOWN
ENSG00000138395	CDK15	1.959216516	0.002574278	0.024931108	-2.106384866	0.001529028	0.010663205	UP	DOWN
ENSG00000182022	CHST15	2.46156993	2.19166E-05	0.000748391	-1.58473528	0.006235001	0.029880317	UP	DOWN
ENSG00000165175	MID1IP1	2.099078393	1.02643E-10	3.67521E-08	-1.946438299	2.06133E-09	1.41938E-07	UP	DOWN
ENSG00000176971	FIBIN	1.825713156	0.00013696	0.00301119	-2.146266679	7.56757E-06	0.000138045	UP	DOWN
ENSG00000107968	MAP3K8	1.398798464	0.004012495	0.034559858	-2.506324799	3.50095E-07	1.0649E-05	UP	DOWN
ENSG00000185507	IRF7	1.724448265	0.000174539	0.003562413	-2.166893198	1.77187E-06	4.19756E-05	UP	DOWN
ENSG00000240764	PCDHGC5	2.137553768	0.000569358	0.008590242	-1.737255583	0.005473647	0.027070548	UP	DOWN
ENSG00000242419	PCDHGC4	1.562897254	0.001309531	0.015308811	-2.287073711	2.21334E-06	5.07085E-05	UP	DOWN
ENSG00000203760	CENPW	1.834285251	4.32594E-06	0.000211768	-1.959450145	2.4437E-07	7.99595E-06	UP	DOWN
ENSG00000068903	SIRT2	1.287558159	0.001774839	0.019033979	-2.499570322	1.20771E-09	9.11751E-08	UP	DOWN
ENSG00000100342	APOL1	2.159817106	0.000109991	0.002571649	-1.582058992	0.004663504	0.024053552	UP	DOWN
ENSG00000183486	MX2	1.489098605	0.001085764	0.013197664	-2.223333317	1.07006E-06	2.73222E-05	UP	DOWN
ENSG00000115267	IFIH1	1.826151483	8.29956E-05	0.002096976	-1.841457518	6.97681E-05	0.000898596	UP	DOWN
ENSG00000141646	SMAD4	1.880289363	0.002127928	0.021668688	-1.781973935	0.003782822	0.020701452	UP	DOWN
ENSG00000137752	CASP1	1.490891218	0.001041712	0.01283651	-2.153026387	2.59469E-06	5.77561E-05	UP	DOWN
ENSG00000120262	CCDC170	1.545056571	0.004850136	0.038937802	-2.045677901	0.000161535	0.001760314	UP	DOWN
ENSG00000092969	TGFB2	1.962298068	0.000115447	0.002659526	-1.617033965	0.001500519	0.01050531	UP	DOWN
ENSG00000075624	ACTB	1.318543775	0.006014546	0.045026459	-2.233541209	3.28366E-06	6.93943E-05	UP	DOWN
ENSG00000196917	HCAR1	1.454968206	0.003550862	0.031672171	-2.095568413	4.80092E-05	0.000667759	UP	DOWN

ENSG00000119508	NR4A3	1.745029962	0.000273968	0.004997627	-1.707876686	0.000310082	0.002955091	UP	DOWN
ENSG00000158352	SHROOM4	1.904922721	9.02312E-08	1.00962E-05	-1.530722377	7.39585E-05	0.000934323	UP	DOWN
ENSG00000164342	TLR3	2.051390134	2.00546E-08	2.82387E-06	-1.356852066	0.000258144	0.002553319	UP	DOWN
ENSG00000184985	SORCS2	2.145716762	2.9632E-07	2.71057E-05	-1.171270298	0.006143116	0.029598694	UP	DOWN
ENSG00000221963	APOL6	1.504366797	7.88239E-05	0.002033444	-1.809537998	2.15037E-06	4.97203E-05	UP	DOWN
ENSG00000185338	SOCS1	1.380426001	0.006195694	0.046052456	-1.92045838	0.000207348	0.002145731	UP	DOWN
ENSG00000197536	C5orf56	1.584165631	2.74698E-05	0.000896488	-1.709321139	1.40707E-05	0.0002348	UP	DOWN
ENSG00000168016	TRANK1	1.744328091	1.39686E-12	1.25039E-09	-1.530157827	6.08272E-10	5.29366E-08	UP	DOWN
ENSG00000139597	N4BP2L1	1.535039456	0.000378802	0.006337985	-1.732021176	4.44234E-05	0.00062412	UP	DOWN
ENSG00000114209	PDCD10	1.877653281	1.09635E-05	0.000443209	-1.322503248	0.001957107	0.012895095	UP	DOWN
ENSG00000110446	SLC15A3	1.32999606	1.0929E-06	7.40333E-05	-1.861029654	1.08504E-11	1.63828E-09	UP	DOWN
ENSG00000183615	FAM167B	1.834800579	0.000188084	0.003747337	-1.353324274	0.001045208	0.007890692	UP	DOWN
ENSG00000167992	VWCE	1.913313009	6.89356E-06	0.000304191	-1.259839355	0.003201778	0.018188884	UP	DOWN
ENSG00000182179	UBA7	1.51452529	0.000123571	0.002795299	-1.646995799	3.04025E-05	0.000454117	UP	DOWN
ENSG00000120093	HOXB3	1.178179052	0.000457425	0.007256261	-1.9349298	9.23305E-09	4.88222E-07	UP	DOWN
ENSG00000101347	SAMHD1	1.815684735	3.63802E-07	3.16609E-05	-1.295443091	0.000284891	0.002752702	UP	DOWN
ENSG00000182578	CSF1R	1.497764402	0.000542526	0.008317742	-1.603736768	0.000169228	0.001825822	UP	DOWN
ENSG00000120075	HOXB5	1.253938428	0.00442422	0.036791192	-1.788096713	4.89181E-05	0.000677395	UP	DOWN
ENSG00000137825	ITPKA	1.79968386	0.000586511	0.008744917	-1.218173142	0.011337602	0.046409691	UP	DOWN
ENSG00000185499	MUC1	1.975966945	2.08385E-06	0.000124356	-1.035755865	0.012309005	0.049393678	UP	DOWN
ENSG00000116667	C1orf21	1.795230746	6.96914E-11	2.64658E-08	-1.157065368	2.81223E-05	0.000425638	UP	DOWN
ENSG00000149929	HIRIP3	1.272404642	0.000124961	0.002816569	-1.676120805	4.53669E-07	1.31911E-05	UP	DOWN
ENSG00000160049	DFFA	1.057575317	0.000846408	0.011072218	-1.886527961	2.24213E-09	1.51883E-07	UP	DOWN
ENSG00000151376	ME3	1.606665786	1.31897E-08	2.06617E-06	-1.290903976	7.0262E-06	0.000130255	UP	DOWN
ENSG00000085276	MECOM	1.757229103	5.00357E-07	3.94369E-05	-1.137053256	0.001367763	0.009750173	UP	DOWN
ENSG00000166801	FAM111A	1.0450607	0.000116097	0.002669581	-1.839713184	1.02946E-11	1.59194E-09	UP	DOWN
ENSG00000125347	IRF1	1.018621594	0.00565074	0.043022524	-1.841432387	5.94996E-07	1.67939E-05	UP	DOWN
ENSG00000181218	HIST3H2A	1.508079659	0.000120071	0.002735879	-1.308209582	0.000756619	0.006008836	UP	DOWN
ENSG00000064042	LIMCH1	1.469700871	3.29381E-11	1.37593E-08	-1.336210718	7.67507E-09	4.2186E-07	UP	DOWN
ENSG00000204839	MROH6	1.182596818	0.003611466	0.032030359	-1.541199581	0.000140522	0.001572338	UP	DOWN
ENSG00000074964	ARHGEF10L	1.57270075	2.01378E-05	0.000704935	-1.133093336	0.002172406	0.013866926	UP	DOWN
ENSG00000104635	SLC39A14	1.325908453	0.000183061	0.003682384	-1.373756035	0.000105409	0.001252119	UP	DOWN
ENSG00000106034	CPED1	1.478318312	0.000157254	0.003323543	-1.166278075	0.002833672	0.016586445	UP	DOWN
ENSG00000184584	TMEM173	1.19030851	2.95222E-05	0.000946221	-1.439935549	4.34676E-07	1.27872E-05	UP	DOWN
ENSG00000025708	TYMP	1.307693634	0.000641652	0.009242735	-1.295934377	0.000696124	0.005675882	UP	DOWN
ENSG00000137507	LRRC32	1.382537049	0.001445937	0.016568844	-1.214174403	0.005162681	0.026056672	UP	DOWN

ENSG00000204209	DAXX	1.381511485	2.60147E-05	0.000864764	-1.213485249	0.000220806	0.002260736	UP	DOWN
ENSG00000077942	FBLN1	1.311841594	0.000316985	0.005552614	-1.250717815	0.00059768	0.004993421	UP	DOWN
ENSG00000145911	N4BP3	1.24374472	0.000664759	0.009434608	-1.318231582	0.00050947	0.004409311	UP	DOWN
ENSG00000164307	ERAP1	1.073050119	5.2688E-05	0.001504068	-1.40718745	1.18953E-07	4.39739E-06	UP	DOWN
ENSG00000113916	BCL6	1.291020882	4.79322E-07	3.80181E-05	-1.17714717	4.94231E-06	9.73853E-05	UP	DOWN
ENSG00000091831	ESR1	1.346229149	0.000525097	0.008104077	-1.119301059	0.009817884	0.041637131	UP	DOWN
ENSG00000111641	NOP2	1.177631441	0.00522573	0.040904967	-1.28692491	0.002393681	0.014769875	UP	DOWN
ENSG00000176974	SHMT1	1.384167111	0.000124272	0.002806091	-1.070509819	0.003152076	0.017963387	UP	DOWN
ENSG00000101871	MID1	1.405274079	0.000106246	0.002521743	-1.048885627	0.003917767	0.021199249	UP	DOWN
ENSG00000006025	OSBPL7	1.114098506	9.40182E-05	0.002296826	-1.320218022	6.15703E-06	0.00011638	UP	DOWN
ENSG00000100307	CBX7	1.159537596	0.000141326	0.003074821	-1.274708204	2.5824E-05	0.000394667	UP	DOWN
ENSG00000048052	HDAC9	1.155854341	0.004896744	0.039036894	-1.248999234	0.002460579	0.015063986	UP	DOWN
ENSG00000122691	TWIST1	1.072130699	0.003200744	0.029315833	-1.294486963	0.000374983	0.003452818	UP	DOWN
ENSG00000162733	DDR2	1.016156733	3.67901E-05	0.001141222	-1.329638564	6.7453E-08	2.72684E-06	UP	DOWN
ENSG00000134291	TMEM106C	1.014481786	0.000903189	0.011573373	-1.276410804	2.85612E-05	0.00043124	UP	DOWN
ENSG00000111077	TNS2	1.091763924	2.61474E-05	0.000866877	-1.179615059	6.07856E-06	0.000115309	UP	DOWN
ENSG00000164010	ERMAP	1.010294532	0.000351624	0.005954808	-1.23858037	1.4981E-05	0.000247681	UP	DOWN
ENSG00000176896	TCEANC	1.000854481	0.005971484	0.044778338	-1.19676095	0.002096163	0.013519872	UP	DOWN

DEGs: differentially express genes; FC: fold change; OE: overexpression; KD: knock-down.